SSC-256

DYNAMIC CRACK PROPAGATION AND ARREST IN STRUCTURAL STEELS

SHIP STRUCTURE COMMITTEE

1976

SHIP STRUCTURE COMMITTEE

AN INTERAGENCY ADVISORY
COMMITTEE DEDICATED TO IMPROVING
THE STRUCTURE OF SHIPS

MEMBER AGENCIES:
United States Coast Guard
Naval Sea Systems Command
Military Sealift Command
Maritime Administration
American Bureau of Shipping

ADDRESS CORRESPONDENCE TO:
Secretary
Ship Structure Committee
U.S. Coast Guard Headquarters
Washington, D.C. 20590

SR-201

16 JAN 1975

This report describes the results of a project that explored the mechanisms of dynamic crack propagation and arrest in ship and other structural steels. The study of fracture has historically been associated with the Ship Structure Committee. Earlier studies contributed substantially to the material success of current ships and led to developments that have supported successful ventures with other structural configurations by other industries.

A prime conclusion of this report is that fracture arrest is governed by the load history of the crack and is thus velocity- and temperature-dependent. It is not solely a material property as the formerly accepted arrest toughness approach had indicated. This is a finding of some consequence that has been picked up and is being investigated further by on-going studies under the sponsorship of the Nuclear Regulatory Commission. The Ship Structure Committee is currently examining the implications of this result to fail-safe design, especially in the use of crack arrestors. These studies will be reported in the future after they are completed.

If you have any comments on this report or suggestions for other projects in this area, they will be most welcome.

W. M. Benkert
Rear Admiral, U. S. Coast Guard
Chairman, Ship Structure Committee

SSC-256

Final Report

on

Project SR-201, "Fracture Arrest Study"

DYNAMIC CRACK PROPAGATION AND ARREST IN STRUCTURAL STEELS

by

G. T. Hahn, R. G. Hoagland,

and A. R. Rosenfield

Battelle Memorial Institute

under

Department of the Navy
Naval Ship Engineering Center
Contract No. N00024-72-C-5142

U. S. Coast Guard Headquarters
Washington, D.C.
1976

ABSTRACT

This is the second of two Ship Structure Committee reports describing a three-year investigation of the crack propagation and arrest characteristics of ship-hull steels. The earlier report (SSC-242), which dealt principally with development of experimental and analytical techniques, is briefly discussed. Results are then presented for the following steels: ASTM-A517F (high strength low alloy), 9% Ni (for cryogenic service), ABS-C and ABS-E (two plates, one of which is high strength and designated EH).

The major material property affecting crack arrest is found to be the dynamic fracture toughness, K_D, which is both velocity- and temperature-dependent. Except for the 9% Ni steel, all of the materials showed an initial decrease of toughness with increasing velocity. Thus, cracks in the steels investigated here display an instability, in that propagation at higher speeds consumes progressively less energy. The negative slope of the toughness/velocity curve is particularly pronounced around the Nil-Ductility Temperatures (NDT) for the ship hull steels. At very low temperatures (e.g. -196°C), the toughness passes through a minimum and then increases with increasing velocity. It appears that this is the most general behavior for cleavage crack propagation.

In contrast, 9% Ni steel fractures by the ductile dimple mechanism and the toughness increases slightly with increasing velocity throughout the velocity range investigated.

CONTENTS

	Page
INTRODUCTION	1
PROGRAM SUMMARY	2
1. Criterion for Fracture Arrest	2
2. Crack Arrest Material Property	2
3. Dynamic Analysis	3
4. The Duplex-DCB Test Procedure	3
5. Current Results	5
6. Implications of the Research	8
7. Recommendations for Future Research	8
MATERIALS	9
PROCEDURE	12
RESULTS	23
A517F	23
9% Ni Steel (A553)	27
ABS-C, -E, and -EH Steels	33
DISCUSSION OF RESULTS	40
CONCLUSIONS	45
ACKNOWLEDGEMENTS	46
REFERENCES	47
APPENDIX A: Analysis of the Side-Grooved DCB Specimen	50
APPENDIX B: Estimation of Size of Largest Tolerable Embrittled Region in Ship Steel at NDT	52

LIST OF FIGURES

FIGURE 1.	Measurement of Crack Arrest	4
FIGURE 2.	Comparison of the Crack Velocity Dependence of Dynamic Fracture Toughness for Various Steels at Various Temperatures	7
FIGURE 3.	Microstructures of the ABS Steels Used in This Investigation	11
FIGURE 4.	Optimization of Heat Treatment of 9% Ni Steels	13

LIST OF FIGURES (Continued)

		Page
FIGURE 5.	DCB-Test Piece Configurations	14
FIGURE 6.	A517F Test Specimen Broken at -196°C	16
FIGURE 7.	Comparison of Experimental Results on Specimen 3Y3 with Analytical Predictions of the Dynamic Beam-on-Elastic Foundation Model	16
FIGURE 8.	Velocity Trace Detected on Transient Recorder	17
FIGURE 9.	Crack Length Versus Time for a Duplex Specimen of SAE4340 Starter Section and ABS-E Steel Test Section	18
FIGURE 10a.	Duplex Specimen of A517F/A553 Tested at -196°C	19
FIGURE 10b.	Fully Side-Grooved Specimen	21
FIGURE 11.	Relation Between Crack Velocity and Dynamic Fracture Toughness for the Double-Cantilever-Beam Specimen	24
FIGURE 12.	Impact Rate and Crack Velocity Dependence of Dynamic Toughness of A517F Steel Over a Range of Temperatures	24
FIGURE 13.	Effect of Crack Velocity on Dynamic Toughness of A517F Steel at -196°C	25
FIGURE 14.	Relation Between Stress Intensity at Crack Arrest and Stress Intensity at the Onset of Rapid Crack Propagation in the Wedge-Loaded DCB Specimen	25
FIGURE 15.	9% Ni Steel	28
FIGURE 16.	Dynamic Fracture Toughness of 9% Ni Steel Compared to that of ASTM-A517F	31
FIGURE 17.	Metallographic Observations of A553 (9% Ni) Steel	32
FIGURE 18.	Dynamic Fracture Toughness and Dynamic Tear Energy Values for Three Ship-Hull Steels	36
FIGURE 19.	Dynamic Toughness as a Function of Crack Speed and Temperature	36
FIGURE 20.	Relation Between Crack Velocity and Dynamic Toughness for Steels Tested Near NDT	36
FIGURE 21.	Fracture Appearance of Ship-Hull Steels	37-38
FIGURE 22.	Crack Arrest Data for Three Ship-Hull Steels	40
FIGURE 23.	A Summary of Direct Measurements of the Dynamic Fracture Toughness of Plain Carbon Steels Below NDT	42

LIST OF TABLES

		Page
TABLE I.	Properties of the Steels Used in this Report	10
TABLE II.	Test Specimen Design Characteristics	22
TABLE III.	Crack Propagation and Arrest Data for A517F Steel	26
TABLE IV.	Dynamic Fracture in Duplex Specimens Consisting of A517F and Ni Steels	29-30
TABLE V.	Crack Propagation and Arrest Behavior of Ship-Hull Steel . . .	34-35
TABLE VI.	Lowest Measured Values of K_D for Steels at Temperatures Close to NDT	43

SHIP STRUCTURE COMMITTEE

The SHIP STRUCTURE COMMITTEE is constituted to prosecute a research program to improve the hull structures of ships by an extension of knowledge pertaining to design, materials and methods of fabrication.

RADM W. M. Benkert, USCG
Chief, Office of Merchant Marine Safety
U.S. Coast Guard Headquarters

Mr. P. M. Palermo
Asst. for Structures
Naval Ship Engineering Center
Naval Sea Systems Command

Mr. M. Pitkin
Asst. Administrator for
Commercial Development
Maritime Administration

Mr. K. Morland
Vice President
American Bureau of Shipping

Mr. C. J. Whitestone
Maintenance & Repair Officer
Military Sealift Command

SHIP STRUCTURE SUBCOMMITTEE

The SHIP STRUCTURE SUBCOMMITTEE acts for the Ship Structure Committee on technical matters by providing technical coordination for the determination of goals and objectives of the program, and by evaluating and interpreting the results in terms of ship structural design, construction and operation.

NAVAL SEA SYSTEMS COMMAND

Mr. C. Pohler - Member
Mr. J. B. O'Brien - Contract Administrator
Mr. G. Sorkin - Member

U.S. COAST GUARD

LCDR E. A. Chazal - Secretary
CAPT D. J. Linde - Member
LCDR D. L. Folsom - Member
CDR W. M. Devlin - Member

MARITIME ADMINISTRATION

Mr. J. Nachtsheim - Chairman
Mr. F. Dashnaw - Member
Mr. F. Seibold - Member
Mr. R. K. Kiss - Member

MILITARY SEALIFT COMMAND

Mr. D. Stein - Member
Mr. T. W. Chapman - Member
Mr. A. B. Stavovy - Member
Mr. J. G. Tuttle - Member

NATIONAL ACADEMY OF SCIENCES
SHIP RESEARCH COMMITTEE

Mr. R. W. Rumke - Liaison
Prof. J. E. Goldberg - Liaison

AMERICAN BUREAU OF SHIPPING

Mr. S. G. Stiansen - Member
Mr. I. L. Stern - Member

SOCIETY OF NAVAL ARCHITECTS & MARINE ENGINEERS

Mr. A. B. Stavovy - Liaison

WELDING RESEARCH COUNCIL

Mr. K. H. Koopman - Liaison

INTERNATIONAL SHIP STRUCTURES CONGRESS

Prof. J. H. Evans - Liaison

U.S. COAST GUARD ACADEMY

CAPT C. R. Thompson - Liaison

STATE UNIV. OF N.Y. MARITIME COLLEGE

Mr. W. R. Porter - Liaison

AMERICAN IRON & STEEL INSTITUTE

Mr. R. H. Sterne - Liaison

U.S. NAVAL ACADEMY

Dr. R. Bhattacharyya - Liaison

INTRODUCTION

There is renewed concern today over the conditions required for the arrest of a fast moving crack. This concern arises from the possibility of large overloads in flawed structures, such as when two ships collide. Rolfe, Rhea and Kuzmanovic [1] have taken the first steps toward a crack arrestor design practice. They conclude that:

> "...the use of steels and weldments with moderate levels of notch toughness combined with properly designed crack arrestors, is recommended as a fracture criterion for welded ship hulls."

Rolfe, et al., have proposed a minimum dynamic test energy (DTE) specification of 600-800 ft lbs (5/8 in. thick DT specimen at 32°F) for crack arrestors with yield strengths from 40-100 ksi. However, it should be clear that these DTE values are a relative measure of material performance and not the absolute measure needed to design a crack arrestor with a specific crack stopping capability. Three absolute measures of arrest performance are currently under discussion:

(1) the arrest toughness, K_a

(2) The toughness associated with the onset of crack extension in a dynamically loaded specimen, K_d, and

(3) the propagating crack toughness, K_D.

The relative merits of these three parameters are examined more fully in Reference [2]. It is sufficient to note here that they are measures of the same property, namely the material's resistance to rapid crack extension. The arrest toughness concept is based on the largely unsupported assumption that the kinetic energy imparted to a structure while the crack is propagating is lost. In contrast the propagating crack toughness is derived from fully dynamic analyses that account for actual contribution of kinetic energy and inertia. The quantity K_d has been proposed as an alternative measure of either K_a or K_D on the basis of a postulated but unproven equivalence between the stress rates generated at the tip of a rapidly loaded stationary crack and an advancing crack.

This report and SSC-242 [3], a report of the earlier work of this program, describe results of a 3-year study of crack arrest in ship steels. The principal aim of the research was to establish a valid measure of arrest performance. The analyses and experiments presented in SSC-242 point to the need for a dynamic analysis, K_D approach. A new method for initiation and arresting fast fractures in small laboratory test pieces over a wide range of temperatures was also demonstrated.

The measurements described in this report were undertaken in order to determine the behavior of commercial ship-hull steels at operating temperatures. Particular attention was focused on the Nil-Ductility Temperature (NDT), as measured by ASTM-E-208, which is a reasonable base point for comparison of structural steels. Data on current ABS grades were normalized according to the respective NDT's of three steels. The higher strength grade, A517F, was tested at and below its NDT while the cryogenic steel A533(9%Ni) was tested above its NDT.

PROGRAM SUMMARY

This section contains a short summary of the findings of Project SR-201 "Fracture Arrest Study" including those presented in SSC-242 and in this report.

1. Criterion for Fracture Arrest

The analyses and experiments described in SSC-242 [3] show that the dynamic, crack tip energy release rate*

$$G_I = \frac{dW^D}{dA} - \frac{dU^D}{dA} - \frac{dT^D}{dA} \tag{1}$$

is the proper basis for formulating the arrest criterion. Energy conservation dictates that the energy release rate must match R_{ID}, the per-unit-area fracture energy, during propagation. Arrest is assured when the minimum value of the fracture energy (this quantity may vary with velocity) exceeds the energy release rate. Accordingly, the criteria for propagation and arrest can be expressed in terms of energy values or in terms of corresponding stress intensity values, K_I, and propagating crack toughness, K_D:**

Propagation

$$R_{ID}(v) = G_I \tag{2A}$$

$$K_D(v) = K_I \tag{2B}$$

Fracture Arrest

$$R_{ID,min} > G_I \tag{3A}$$

$$K_{D,min} > K_I \tag{3B}$$

2. Crack Arrest Material Property

The criteria given above seem to show that the material property governing arrest is $R_{ID,min}$ (or $K_{D,min}$), the minimum in the energy- (or toughness-) crack velocity dependence. The arrest process is actually more complicated

---

* Where U is the strain energy in the cracked structure, T is the kinetic energy and W is the work performed on the structure by the surroundings. A is the area of crack advance and the superscripts D emphasize that the quantities require dynamic analyses.

** Note that this represents a change in nomenclature from that employed in SSC-242. The term K_D, which was formerly used to designate the propagating crack toughness is now reserved for the toughness associated with one extension of a stationary crack under dynamic loading. For the balance of this report SI units will be used:
$1 MNm^{-3/2} = 0.9\ ksi\sqrt{in}$; $1J = 0.738$ ft-lb; $1J/m^2 = 5.71 \times 10^{-3}$ in-lb/in^2.

because the values of U, T, and W, their derivatives, and consequently, the instantaneous value of G_I are influenced by the history of fracture energy dissipation during the period the crack is running. As a result, the point of arrest is governed by $R_{ID}(v)$ or $K_D(v)$, specifically the portion of the fracture energy-crack velocity dependence sampled by the crack during the entire propagation event preceding arrest. The analysis also suggests that $R_{ID,min}$ and $K_{D,min}$ reduce to G_{Ia} and K_{Ia}, the so-called arrest energy and toughness [4] in situations where the kinetic energy and dynamic effects are negligible.

3. Dynamic Analysis

Existing controversies about crack arrest are not concerned with the criteria (Equations 3A and 3B) but arise from the dearth of dynamic analyses and the uncertainty about the relative contributions of $\frac{dU^D}{dA}$, $\frac{dT^D}{dA}$, and $\frac{dW^D}{dA}$. In SSC-242 [3], Kanninen derived a fully dynamic analysis of propagation and arrest in a wedge-loaded rectangular-DCB specimen with finite dimensions. This analysis reveals that the kinetic energy release rate $-\frac{dT^D}{dA}$ is comparable to the strain energy release rate $-\frac{dU^D}{dA}$ in the latter stages of propagation in this test piece. Substantial differences between $-\frac{dU^D}{dA}$ and the statically calculated value are also encountered. It appears that dynamic effects, in general, cannot be neglected.

4. The Duplex-DCB Test Procedure

Substantial progress was made towards a practical method of measuring the crack arrest property $R_{ID}(v)$ or $K_D(v)$, of ship steels. The work began with the wedge-loaded, rectangular DCB-specimen. This configuration was selected because it makes it possible to initiate and arrest cracks within the confines of the test piece.

The essential features of the experimental procedures are illustrated in Figure 1. In brief, the specimen containing a blunt starter notch is wedge-loaded, in order to initiate rapid crack propagation. Crack velocities are measured using a grid of conducting strips electrically insulated from the sample. The signals corresponding to the breaking of individual strips are recorded electronically and translated into a crack length vs. time record. Toughness values are calculated from the analysis given in SSC-242.

In the course of the program the following refinements were made:

(i) Duplex DCB-Specimen. As discussed more fully in SSC-242 [3], the capabilities of the DCB specimen were greatly enhanced by attaching a high strength/low toughness "starter section" to the "test section" by electron beam welding. This arrangement, the so-called "duplex" DCB specimen, makes it possible to initiate the fast fracture at virtually any temperature, even above the transition temperature of the test plate. The higher yield strength of the starter section reduces the specimen size requirements in proportion to ($\sigma_{Y,\text{starter section}}/\sigma_{Y,\text{test section}}$) [2], typically by an order of magnitude.*

* σ_Y is the yield strength.

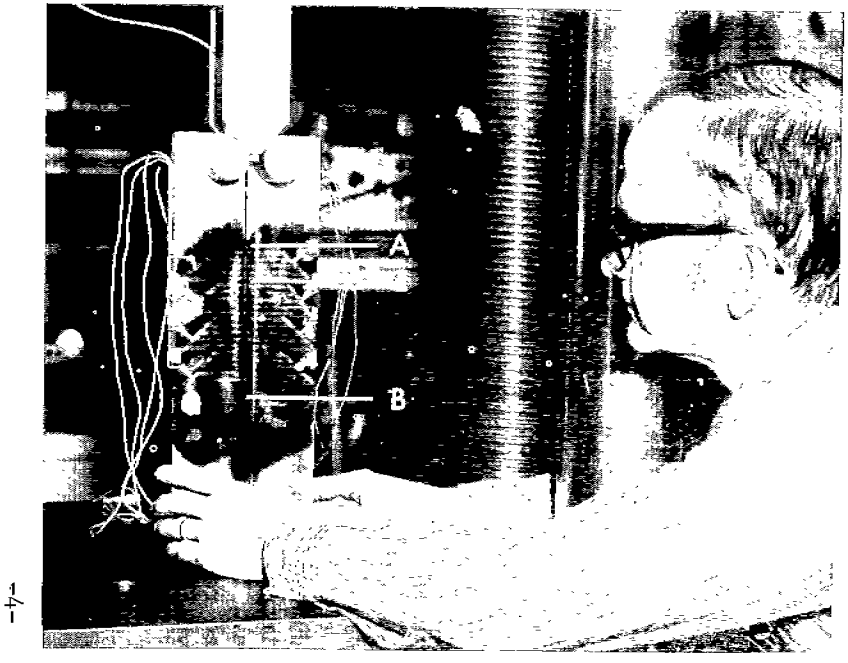

(a)

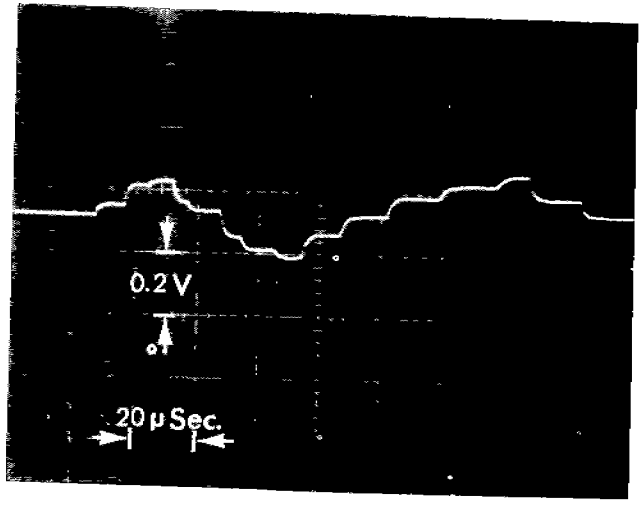

(b)

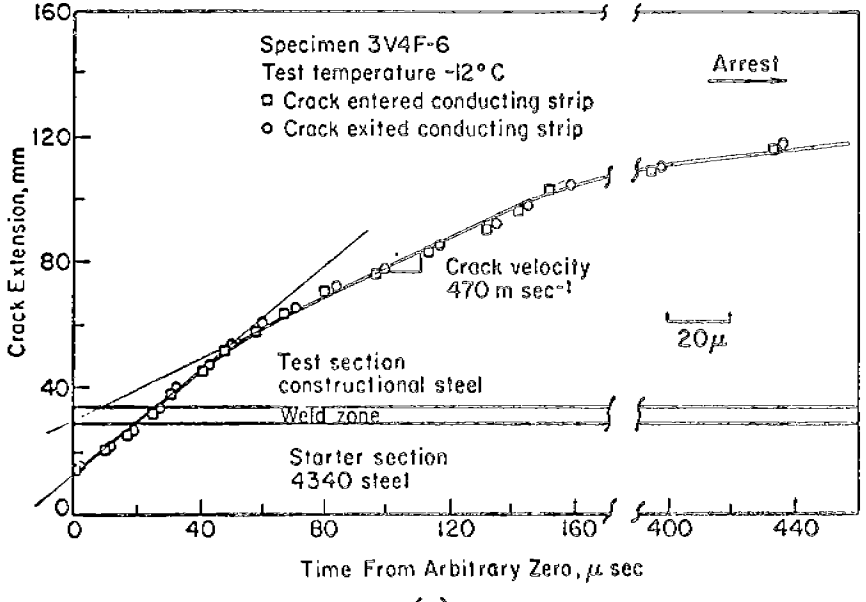

(c)

FIGURE 1. MEASUREMENT OF CRACK ARREST: (a) Wedge-loaded laboratory test piece. The points of fracture initiation (A), crack arrest (B), and the weld line between the starter section and the test material (C), are identified. The horizontal conducting strips are also visible in the photograph. (b) Record of the variation of grid voltage with time during crack propagation, and (c) graph of the change of crack length with time derived from (b).

(ii) Welding Problems. Problems of cracking, particularly delayed cracking of the electron beam welds, were encountered with some of the ship grades. The problem has now been resolved by preheating and postheating. Specimens up to 50 mm- (2 in.-) thick have been prepared and tested successfully.

(iii) Crack Velocity Measurement. The technique for measuring the velocity of the fracture in the test piece was extended to lower test temperatures. In the case of the A553 (9% Ni) grade velocities were measured successfully at both -160°C and -196°C.

A major problem encountered on another structural steel investigated at Battelle-Columbus Laboratories was the strong tendency for cracks to branch in the DCB test piece after entering the test sections. It was necessary to eliminate the branching because the propagating branched crack cannot be analyzed at this stage. Larger compression loads (obtained by increasing the wedge angle) were employed but did not suppress the branching. Deep side grooves* did prove to be effective and were adopted as an interim solution. A result obtained for the A517F grade showed that the side grooves do not alter the mechanics of propagation of flat fracture, though a correction must be made for the reduction in the area of crack advance.** However, the side grooves do inhibit the formation of shear lips near the plate surface at temperatures close to and above NDT since the shear lips consume more energy than the flat fracture in the interior. The measurements derived from side-grooved specimens therefore understate the K_D values of relatively thin plates above the NDT, and should be regarded as lower bound values.

The present side-grooved DCB-specimens are well suited for measuring the toughness values appropriate for heavy sections, e.g., plane strain. A further refinement, possibly in the method of loading, that will eliminate branching without interference by the formation of shear lips is needed to extend the usefulness of the test procedure to relatively thin ship plates above NDT.

Currently the specimen design is capable of measuring dynamic fracture toughness values up to $\sim$250 $MNm^{-3/2}$. This is probably insufficient for steels which exhibit extensive shear lips (e.g., 25 mm thick plates tested above NDT). Scaling up the width of the specimen and changing the geometry of the test section to more of an I-shaped profile should more than double the capacity. The width increase would allow more elastic energy to be stored in the specimen prior to crack initiation. At the same time, the reduced cross section would provide a smaller thickness and less energy absorption per unit length of crack advance.

5. Current Results

For the steels tested here, K_D has been found to be a complex function of three factors:

(a) metallurgical variables, such as composition,

---

* The grooves on each side of the test piece were cut to a depth corresponding to 30% of the cross section.

** See Appendix A.

(b) test temperature,

(c) crack velocity.

Thus, for any given steel, a three-dimensional plot of toughness, temperature, and velocity would be needed to provide a complete characterization of resistance to fast fracture.

Not only does the absolute value of toughness depend on test temperature, but also the velocity dependence, as shown in Figure 2. This figure summarizes the major results reported here. The three curves are qualitatively different:

(a) The crack-resistant 9% Ni steel has a high static fracture toughness (i.e., K_D (v = 0) = K_{Ic}) and toughness increases monotonically, although slowly, with crack speed. At a speed of 1000 m/s, this steel has the highest toughness of all, even when tested at -196°C.

(b) The A517F and ABS-C grades tested at -196°C, well below the ductile/brittle transition temperature, initially exhibit a small decrease of toughness, which passes through a minimum at modest speeds and then increases at a moderate rate.

(c) The ABS grades (C, E, and EH) and the A517F grade tested at NDT* show a sharp decrease in toughness. It is not established whether there is a minimum in the toughness/velocity curve, although some indirect evidence suggests that the lowest value in the NDT curve of Figure 2 is close to the minimum.

The behavior of the steels at NDT is particularly important because it represents a strong tendency for unstable fracture, in that the faster a crack travels, the less energy it consumes. Balancing this are the rather high toughness level and the apparently extremely high initiation toughness. In a practical situation, the initiation toughness can be "bypassed" by the presence of welds with high residual stress and localized regions of low toughness which can serve as sites for initiation. The research also shows that NDT is a useful reference temperature for comparing different steels, a factor which may become important in translating the data here to practical terms.

The K_D values at NDT reported here correspond to fracture energies in the range of 50-200 KJ/m^2. In contrast, the dynamic tear energies of 25.4 mm thick ship steel are on the order of 250-500 KJ/m^2 at NDT.[5] The difference arises at least partly from the presence of side grooves in the DCB specimens tested on this program. The side grooves inhibit shear lip formation which begins to make an important contribution to fracture energy in 25.4 mm thick samples at temperatures around NDT.[5] As the temperature is raised above NDT, the dynamic tear energy rises more steeply than the fracture energy measured on side-grooved specimens because of the increasing importance of shear-lip formation in the full-thickness sample. For this reason the side-grooved specimen provides a measure of crack propagation resistance which is likely to be conservative at NDT and to become increasingly more conservative as the temperature is raised above NDT.

---

* The nil-ductility temperature as measured by ASTM-E-208.

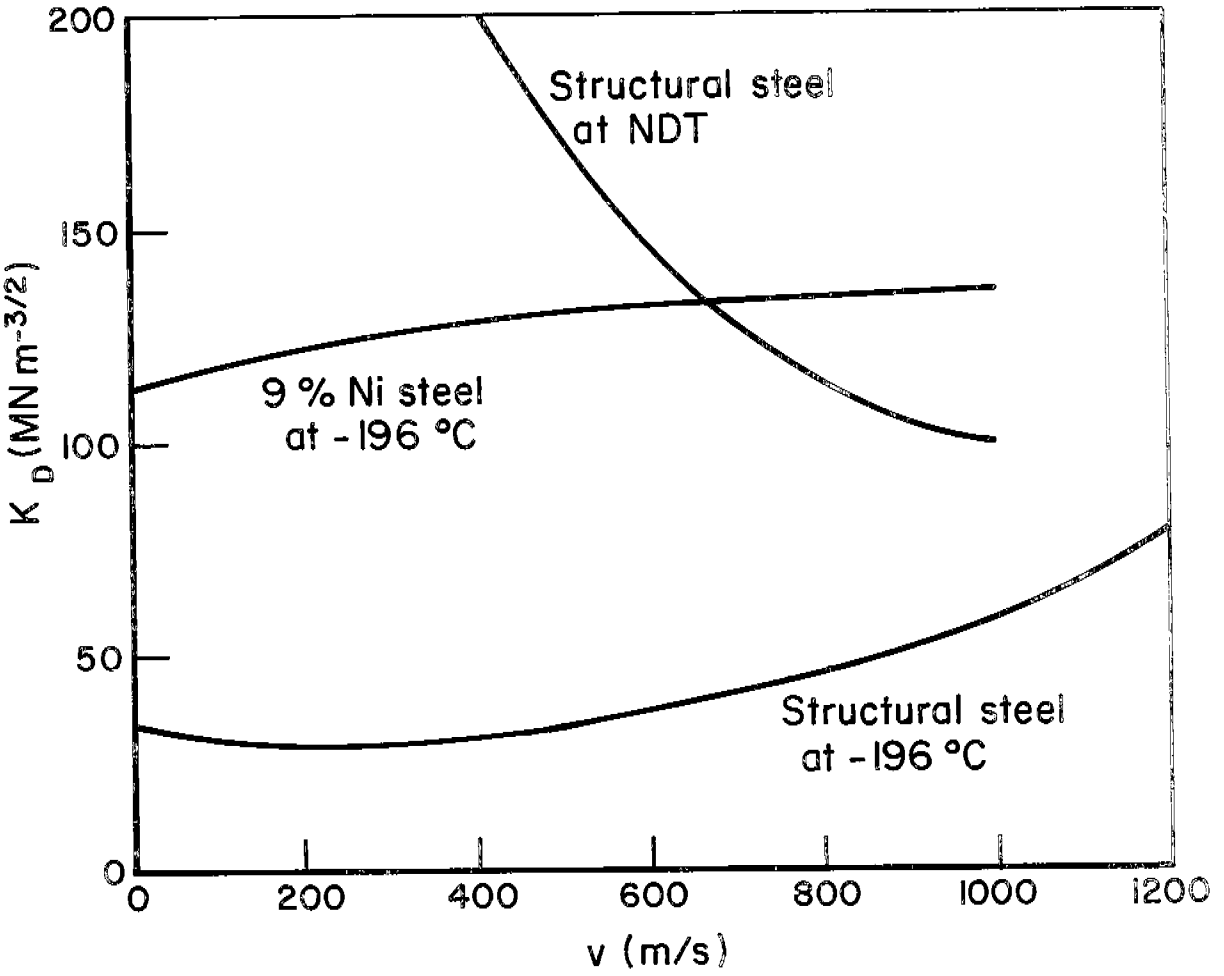

FIGURE 2. COMPARISON OF THE CRACK VELOCITY DEPENDENCE OF DYNAMIC FRACTURE TOUGHNESS FOR VARIOUS STEELS AT VARIOUS TEMPERATURES

6. Implications of the Research

This research points the way towards estimating how far a crack will travel before it arrests. An estimate of the largest possible propagating crack which could be arrested by the steels studied here at very low temperature where shear lip formation is minimal can be made:

$$a \approx \left(\frac{K_D}{\sigma} \right)^2 \tag{4}$$

where a is the half crack length, and σ is the applied stress. Using typical values, $K_D \geq 100$ $MNm^{-3/2}$ and $\sigma = 170$ MNm^{-2}, a becomes 110 mm. Larger cracks would propagate catastrophically.

A number of additional steps need to be taken in order to translate this simple calculation into a practical approach to ship safety. These steps would eliminate the simplifying assumptions:

(1) Treating the ship as an infinite center-cracked panel. While this assumption was made in a recent failure analysis,[6] its justification is not clear. For impact loads, this assumption is probably very bad. The deck can be treated as a center-cracked panel for hogging loads since the form of the stress intensity is the same as for beams in bending. However, the bulkheads would act as stiffeners. Basically, what is needed is a fully-dynamic solid-mechanics analysis of the ship hull structure containing a crack and subjected to realistic loads.

(2) An initial flaw size has to be specified. Probably the most conservative assumption would be to treat an entire welded seam as the flaw. This would result in starting flaws 1-2 m long and K_Q values in the range 250-350 $MNm^{-3/2}$.

(3) The conservative value of dynamic fracture toughness is the minimum in the toughness/velocity curve. Further experimentation is needed to determine the exact value of the minimum. Also research is required to determine whether there is a relation between values obtained in simpler, cheaper tests, such as Charpy, and those described here, which characterize the running crack.

The approach described here can also be applied to the design of arrester plates. In this case, the equations are much more complex and the dynamic toughness of both the hull plate and arrestor plate must be known as functions of velocity.

7. Recommendations for Future Research

1. Develop methods for testing thin sections. In this context, "thin" refers to plates where the constraints due to plane strain have broken down and shear lip formation is allowed. Such experimentation will allow for more realistic fracture toughnesses to be measured above NDT. In order to accomplish this objective, the measuring capacity of the specimen would be increased further than has been done on the current project.

2. Develop a fuller description of the variation of the dynamic fracture toughness associated with a rapidly propagating crack. The results developed in this program need to be extended over a wider velocity range, particularly at anticipated service temperatures. At these temperatures crack propagation will be mixed-mode, a combination of flat fracture and shear lips.

3. Measure the resistance of weld to rapid crack propagation. While cracks in current ship-hull grades tend to traverse the base plate, extensive crack propagation along welds is anticipated at higher strength levels. A simple modification of the duplex DCB specimen can provide such data.

4. Relate the mechanics of the DCB specimen to other geometries. A satisfactory description of fast fracture requires a fully dynamic analysis of the geometry and loading involved. Such an analysis should be applied to laboratory specimens such as dynamic tear and to ship hull structures under impact loading, for example.

MATERIALS

Five steels were chosen for investigation as being of current of potential interest for ship hull applications. Relevant properties are listed in Table 1.

The three ABS grades are the same plates investigated by the Naval Research Laboratory [5] in their survey to determine whether currently available ship plate meets the fracture-safety criterion suggested by Rolfe, et al.[1] Microstructures of these steels are given in Figure 3. Note particularly that there is a correlation between fine grain size, low NDT, and high dynamic tear energy at NDT.

The A517F is a high-strength quenched and tempered steel which is of possible future interest. Preliminary dynamic toughness data had previously been obtained in this laboratory[9] and extensive impact-test results have been reported by Rolfe and co-workers [7,10].

The 9%Ni steel is being used for cryogenic applications, such as LNG tankers. Its nil-ductility-temperature is reported to be below the boiling point of liquid nitrogen. [8] More precise measurements of low-temperature toughness have been difficult to obtain. Attempts to measure K_{Ic} at -196°C have been complicated by excess plasticity,[11,13] but values of K_Q corresponding to extension of a fatigue pre-crack and based on 5% secant offset are in the range 110-140 $MN/m^{-3/2}$. As a result, the constraint associated with plane-strain behavior is lost beyond rather modest thicknesses (25-40 mm), and side grooves are required to produce flat fracture.

The resistance to rapid crack propagation and to crack arrest is very poorly defined. Charpy impact energies in excess of 50J (37 ft-lb) at temperatures below -150°C have been reported by several authors. [12,14] To the extent that Charpy energy related to crack propagation resistence, this is encouraging evidence that this steel has adequate toughness. At the same time, toughness appears to be extremely sensitive to heat treatment. Figure 4,

TABLE I. PROPERTIES OF THE STEELS USED IN THIS STUDY

	Steel Identification Code		Composition (Wt.%)						Mechanical Properties				
	Battelle	NRL	C	Mn	P	S	Si	Other	YS(MNm^{-2})	UTS(MNm^{-2})	RA(%)	NDT(°C)	Dynamic Tear Energy at NDT (J)
ABS-C[f]	4F	U-12[a]	0.15	0.82	0.008	0.028	0.25	-	270[a]	440[a]	67.4[a]	-12[a]	542[a]
ABS-E[f]	4G	U-30[a]	0.07	1.23	0.007	0.019	0.19	-	282[a]	423[a]	78.6[a]	-23[a]	732[a]
ABS-EH[f]	4H	U-32[a]	0.18	1.41	0.005	0.019	0.26	-	376[a]	533[a]	72.9[a]	-51[a]	1031[a]
A517F[f]	3Y	-	0.15	0.80	0.008	0.013	0.26	0.86Ni 0.48Cr 0.42Mo	810[b]	886[b]	69[b]	-40[d]	-
A533[g]	4A	-	0.06	0.64	0.01	0.013	0.20	9.04Ni	1075[c]	1185[c]	62[c]	< -196[e]	-

(a) Data from Naval Research Laboratory, Reference [5].
(b) -78°C.
(c) -196°C.
(d) Reference [7].
(e) Reference [8].
(f) As received.
(g) Austenitized 800°C, 35 min, WQ; tempered 605°C, 31 min, Air Cooled.

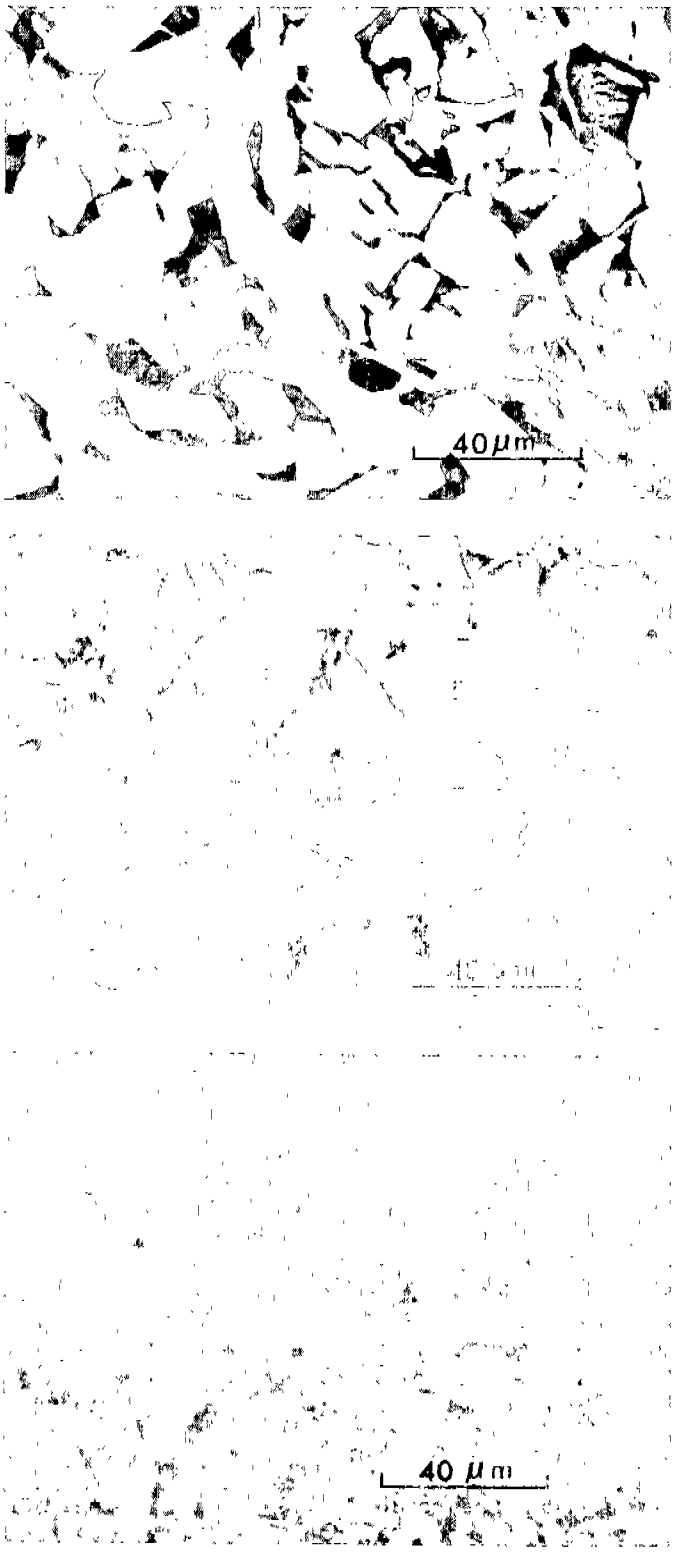

(a) ABS-C

(b) ABS-E

(c) ABS-EH

FIGURE 3. MICROSTRUCTURES OF THE ABS STEELS USED THIS INVESTIGATION

taken from the data of Ooka, et al, [15] shows the extent of this effect. Note particularly the shaded band in Figure 4b, defining the allowable tempering temperature according to ASTM-A553-72, one of the specifications covering the steel. Variations in Charpy energy of almost a factor of three fall within this band.

While the exact reasons for the variability of toughness are not clear, they must arise from the special effects of heat treatment in 9% Ni steels. Marschall, et al[16] have pointed out that austenite begins to form upon heating these steels to temperatures ∿450-500°C. Thus, tempering at higher temperatures will result in partial reaustenization, as is shown in Figure 4a. The austenite retention varies with reheating temperature: in steels heated above ∿565°C, martensite formation is more complete after quenching to -196°C than to 25°C, while the austenite formed at and below ∿565°C is more stable, in that cooling below room temperature provides no additional martensite formation.[16] This phenomenon complicates the interpretation of the temperature variation of toughness, since, in many cases, the steel may undergo partial phase transformation in cooling to the test temperature. Furthermore, these steels exhibit transformation-induced plasticity[15] ("TRIP" effect) which should depend on the amount and nature of the austenite present.

The practical effect is that the impact energy does not depend uniquely on austenite content as shown in Figure 4a. (Note that the peak in the impact energy versus tempering temperature curve anticipates the peak in the retained austenite versus tempering temperature curve.) This observation precludes defining a single relation between microstructure and toughness, just as the sensitivity to heat treatment complicates the problem of comparing results obtained in different laboratories.

Notwithstanding these difficulties it is important to define the crack propagation resistance and crack arrest capability of 9% Ni steel. To this end, a commercially produced and heat-treated 12.7 mm thick plate satisfying ASTM-A553 was obtained so that the dependence of fracture toughness on crack velocity could be measured.

PROCEDURE

The wedge-loaded double-cantilever-beam (DCB) specimen was used in these experiments and the results were analyzed with the beam-on-elastic-foundation model. Both the experimental and analytical procedures have been described extensively elsewhere.*[9,17-19] Over the course of the program several different specimen designs were adopted depending on the particular steel and test temperature. Several of the designs used on A517F early in the program are sketched in Figure 5. The ordinary specimen (Figure 5a) contains a blunt starter notch which allows the specimen to store excess elastic energy before crack extension. Once the crack begins to propagate, this oversupply becomes available to drive the crack rapidly. Eventually the crack exhausts the supply

* Modifications were that for temperatures below -78°C, the velocity measuring grid was insulated from the specimen by A12 Epoxy (Techkits, Demarest, N.J.), and that in the last year of the program velocity traces were recorded on a Biomation Transient Recorder.

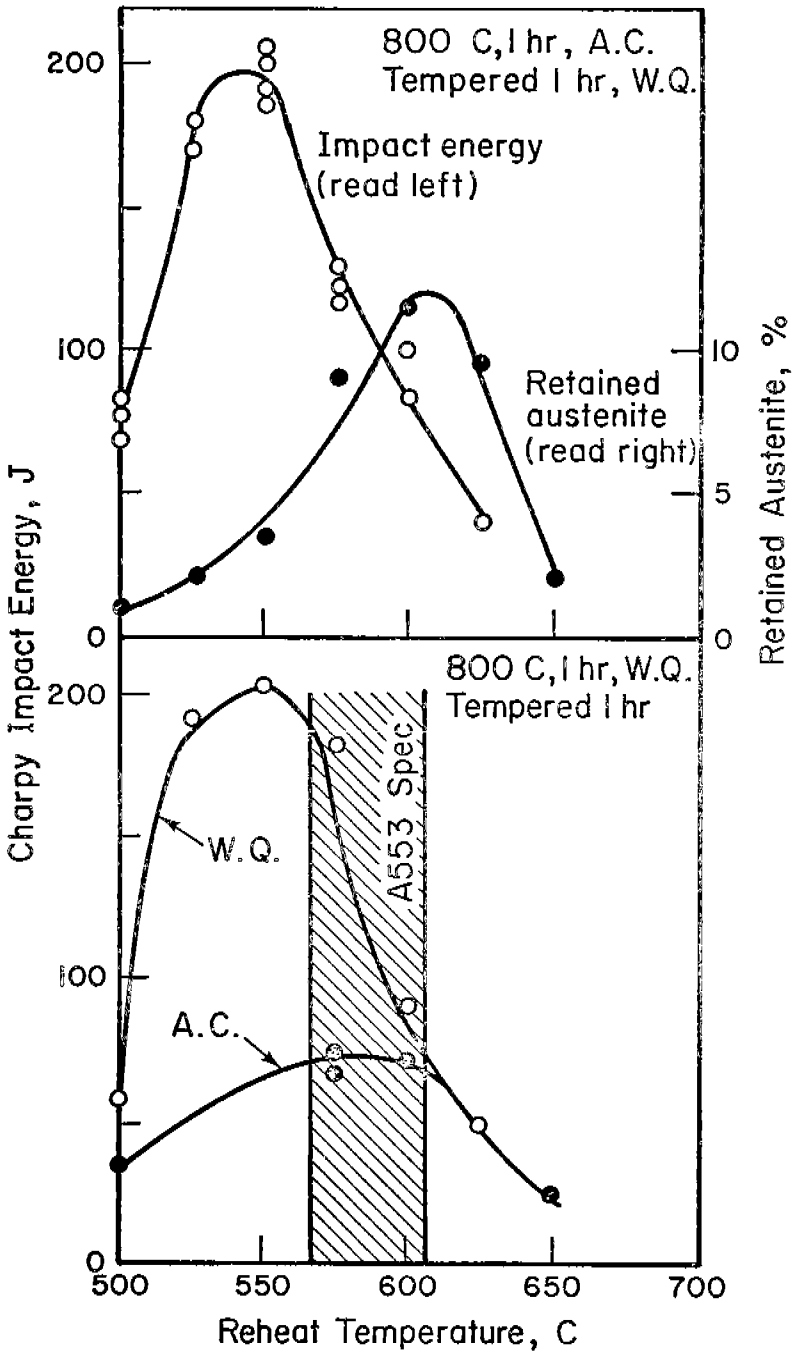

(a) Variation of impact energy and retained austenite with 'tempering' temperature.

(b) Effect of quenching rate after 'tempering' on impact energy.

FIGURE 4. OPTIMIZATION OF HEAT TREATMENT OF 9% Ni STEELS
Data of Ooka, et. al. [6] at -196°C.

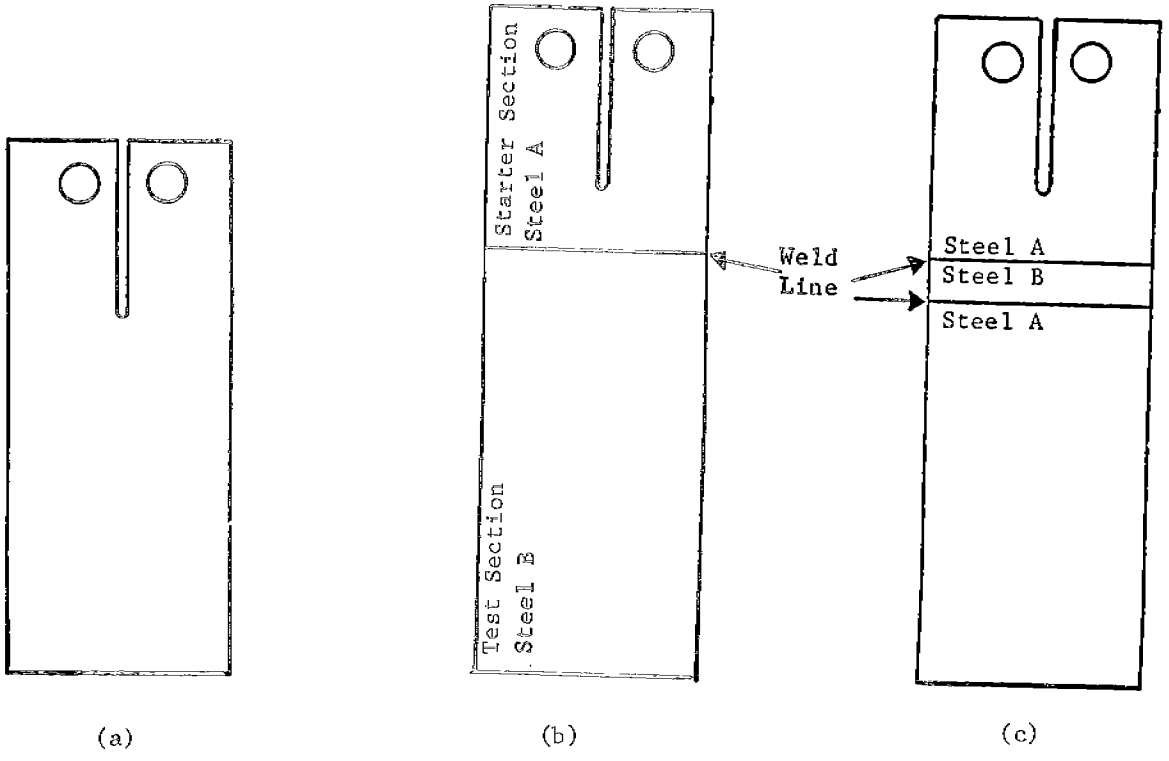

FIGURE 5. DCB-TEST PIECE CONFIGURATIONS: (a) ordinary (homogeneous) DCB-specimen, (b) duplex DCB specimen, and (c) crack arrestor DCB specimen.

of excess strain energy and arrests. Figure 6 shows an actual sample while Figure 7 shows its crack length vs. time dependence. Velocity was measured by recording the rupturing of individual lines of the vapor-deposited grid evident on the specimen surface in Figure 6. A time trace representative of the latter stages of the program, is shown in Figure 8.

The ordinary DCB specimen is appropriate for high-strength/low-toughness materials, such as SAE4340 steel [18] or structural steel at very low temperatures. However excessive yielding will occur before rapid crack propagation can be initiated when [20]

$$h \geq 1.5 \left(\frac{K_Q}{\sigma_Y} \right)^2 \tag{5}$$

where h is the specimen half-height, K_Q is the effective stress intensity at the onset of fast fracture, and σ_Y is the yield stress. For steels of low yield strength, the size requirements imposed by Equation (5) are excessive. This problem has been overcome by developing the duplex specimen (Figure 2b) in which a high-strength low-toughness starter section is electron-beam welded to the steel being tested. A rapid crack, initiated in the starter section, propagates into the test section and eventually arrests. A plot of crack length vs. time for a duplex specimen is given in Figure 9. As before, [3,21] a steady-state crack velocity is achieved in the starter section. After the crack has penetrated into the test section, a new steady-state velocity, characteristic of the higher toughness structural steel, is achieved. Finally, the crack beings to decelerate and arrest. It is believed that this process occurs essentially under fixed-grip conditions.

After the crack has ostensibly arrested for a few hundred microseconds, a small additional jump is observed. It is believed that this jump is associated with the machine "catching-up" and releasing additional stored energy into the specimen. While the jump had not been detected earlier,[3,28] it was found in a number of the present experiments due to the higher resolution brought about by the introduction of the transient recorder.

The arrestor specimen, shown in Figure 5c, is a laboratory simulation of an arrestor plate in a ship. It consists of a strip of high-toughness steel welded to two plates of low-toughness steel.

Initial attempts to use SAE4340 for the low-toughness starter-section in the 9% Ni steel experiments were unsuccessful because of severe weld cracking. This difficulty was overcome by using ASTM-A517F instead. Since the experiments were carried out a temperatures $\leq -150°C$, A517F steel [9] was appropriate for the low-toughness starter section. Initial root diameter of the starter notch varied from 0.28 to 1.85 mm to insure a range of crack speeds in the various specimens.

In the earliest experiments on 9% Ni steel the crack arrested at the weld line and did not penetrate into the test section. To overcome this problem the partially side-grooved specimen of Figure 10a was devised. This design has three advantages:

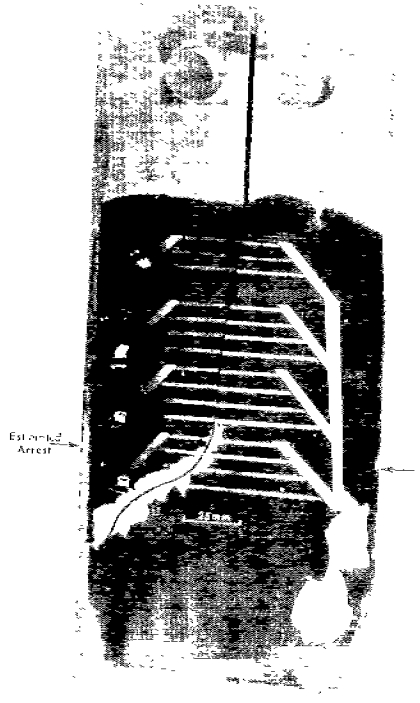

FIGURE 6. A517F TEST SPECIMEN BROKEN AT -196°C. Specimen number 3Y3. K_q/K_{Ic} = 2.44

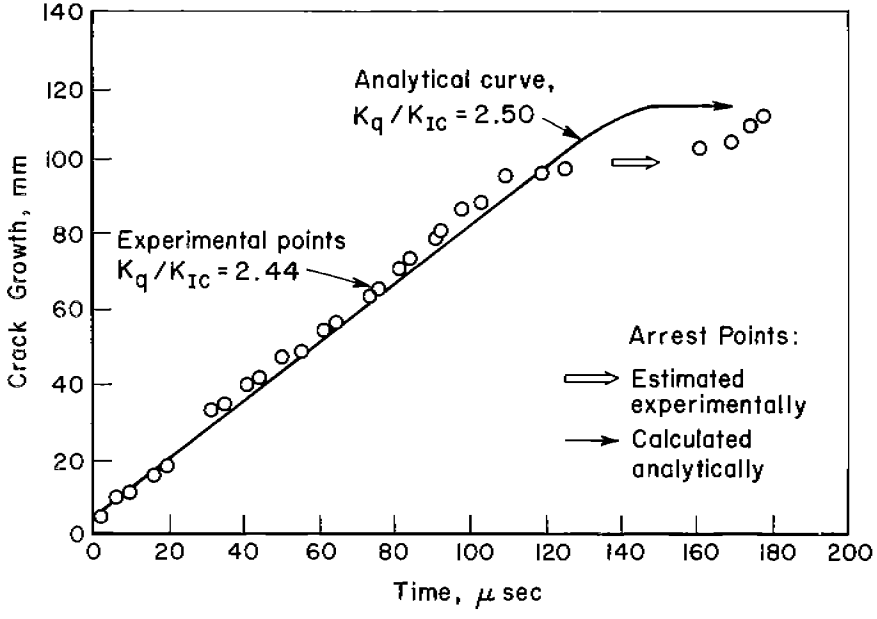

FIGURE 7. COMPARISON OF EXPERIMENTAL RESULTS ON SPECIMEN 3Y3 WITH ANALYTICAL PREDICTIONS OF THE DYNAMIC BEAM-ON-ELASTIC FOUNDATION MODEL [19]

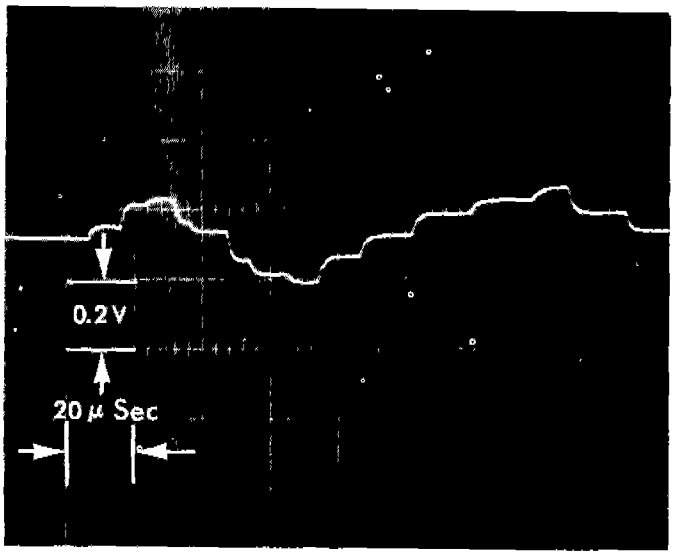

FIGURE 8. VELOCITY TRACE DETECTED ON TRANSIENT RECORDER
ABS-E Steel Tested at -12°C.

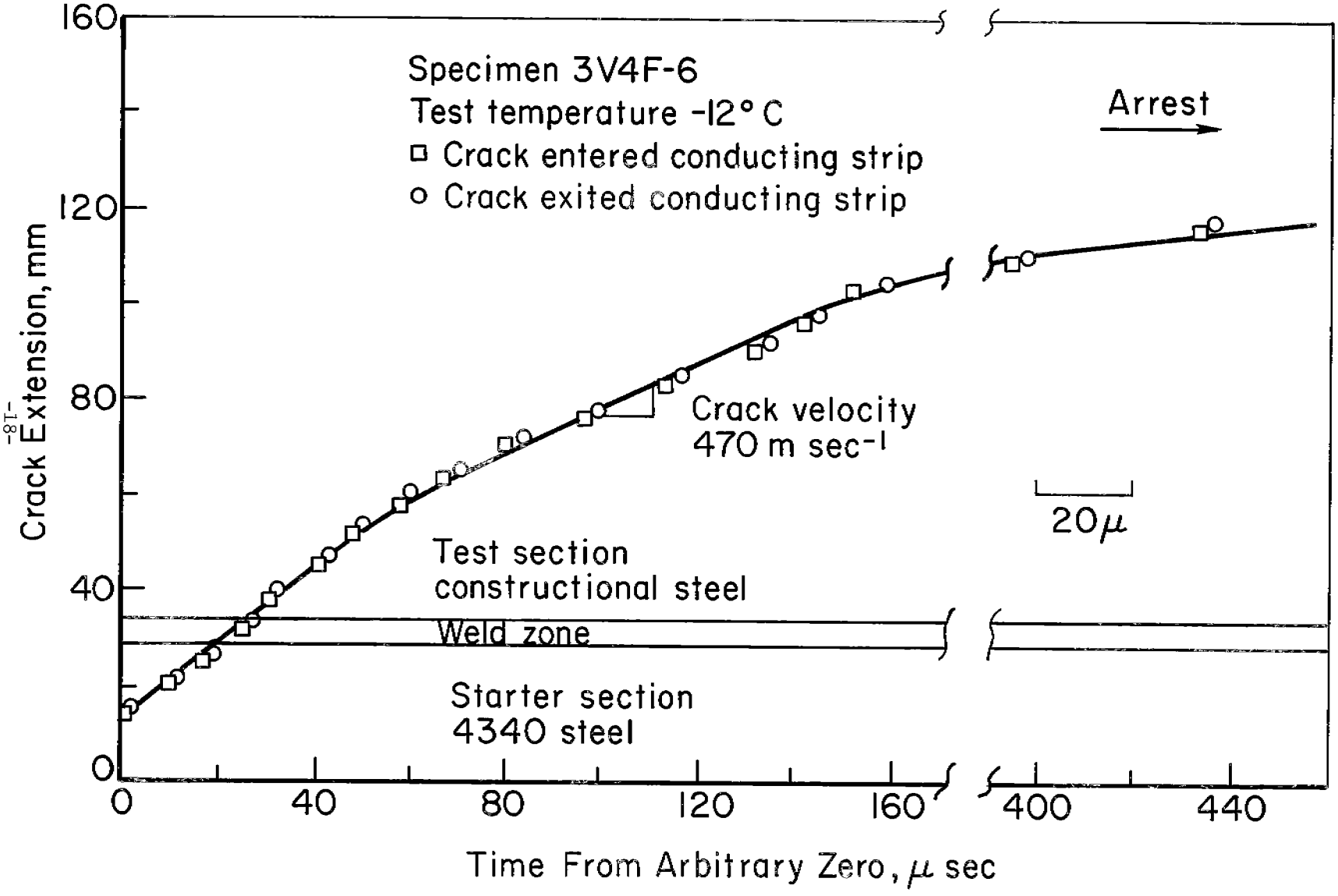

FIGURE 9. CRACK LENGTH VERSUS TIME FOR A DUPLEX SPECIMEN OF SAE4340 STARTER SECTION AND ABS-E STEEL TEST SECTION.

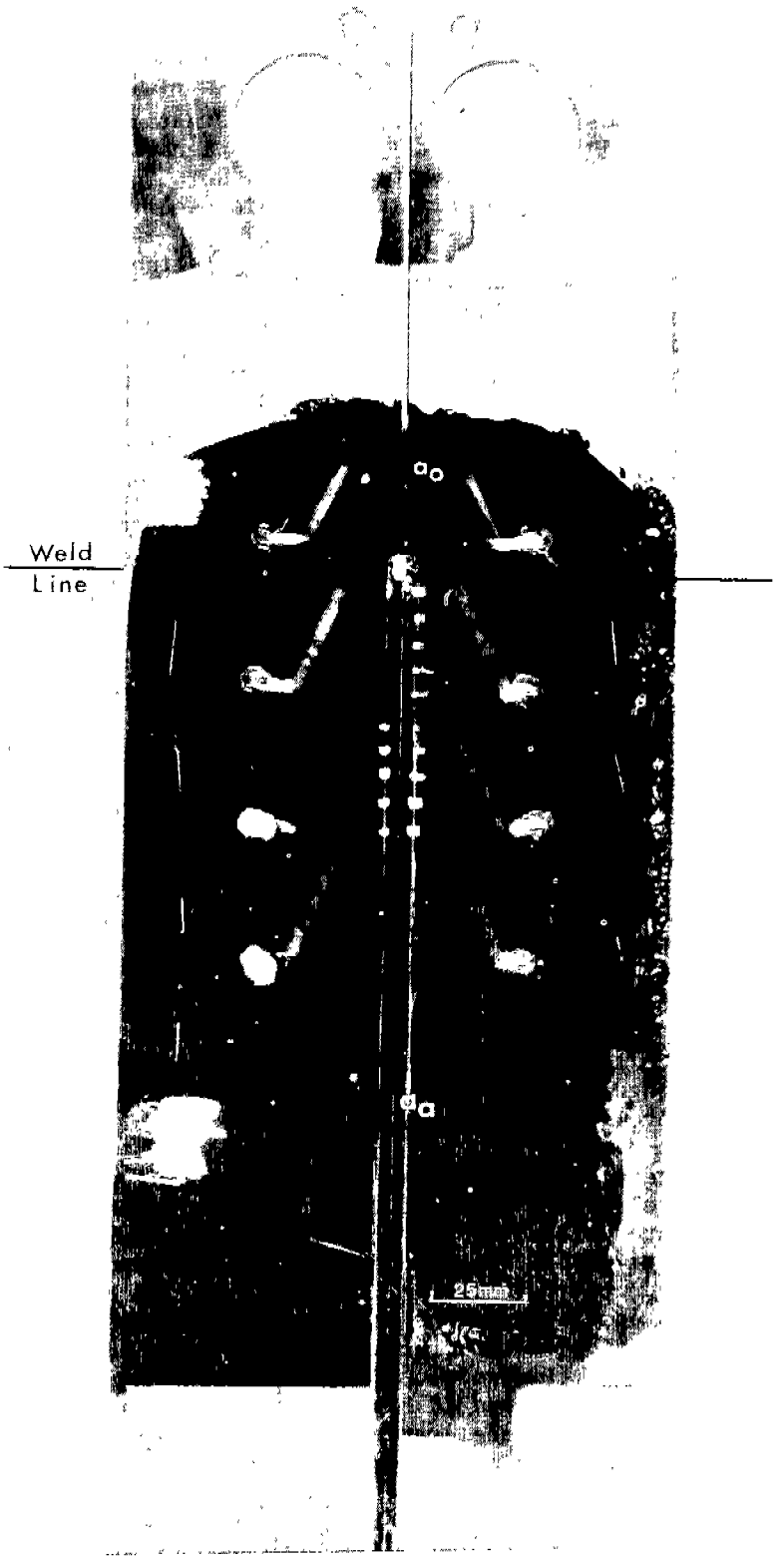

FIGURE 10. DUPLEX SPECIMEN OF A517F/A553 TESTED AT -196°C. Introduction of side-grooves allows crack propagation into the 9% Ni Steel. Crack arrested in 9% Ni Steel at point marked a_a.

(1) The reduced cross section extends the measuring capacity of the specimen to higher toughness levels.

(2) The grooves inhibit shear lip formation so that the reported toughnesses should approximate plane-strain values. Because of this, the behavior revealed here in thin sections should be a good approximation to thick section properties.

(3) The grooves also promote straight-line crack travel.

Straight-line crack travel is promoted when the smallest possible included angle of the side-groove is used. However, as the included angle is reduced it becomes progressively more difficult to deposit the velocity measuring grid. The compromise adopted was to use a 90° angle for the side containing the grid and a 60° angle for the opposite side.

While this procedure was successful for the 9% Ni steels, when it was applied to the ABS grades a problem was encountered with the crack deviating from a straight-line path in the SAE4340 steel starter section and not entering the test section. To overcome this, fully side-grooved specimens were adopted, in which the grooves ran the entire length of the specimen (Figure 10b). This design also had the advantage of cutting machining costs considerably by eliminating an EDM operation. In addition, the problems with weld cracking were solved by using a preheat of 260°C and a postheat of 315°C without cooldown.

Table 2 lists the designs of the individual specimens tested in this program. The duplex, fully-side-grooved DCB specimen was found to be the most suitable design for these experiments. However, this design has two drawbacks:

(1) Since shear lip formation in the test section is inhibited, full thickness behavior is not reproduced for conditions where there is a large shear lip contribution to toughness. The most pertinent example of this is 25 mm thick plate at and above NDT.

(2) The test-section-only side-grooved specimen allows the toughness range investigated to be extended to higher levels (see Appendix A).

There were several early experiments on the A517F steel at -196°C for which the crack velocities were not measured, (series Z in Table 2). In this case they were interpolated from a plot of K_Q vs velocity for all of the specimens tested at -196°C for which velocities were measured.

In some of the specimens tested at -196°C crack arrest occurred by a perpendicular deviation of the crack from its original path so that one arm broke off the specimen (Figure 6). However, this occurred after the crack had begun to decelerate. As shown in Figure 7 the arrest point calculated from the model is close to the deceleration region. As a result the reported arrest values represent deviations of the crack an amount 10-20% of the beam height from its original path. The veering is due to lateral movement of the loading pins which relieves the compressive load due to the wedge, and was eliminated in the later tests by the use of side grooves.

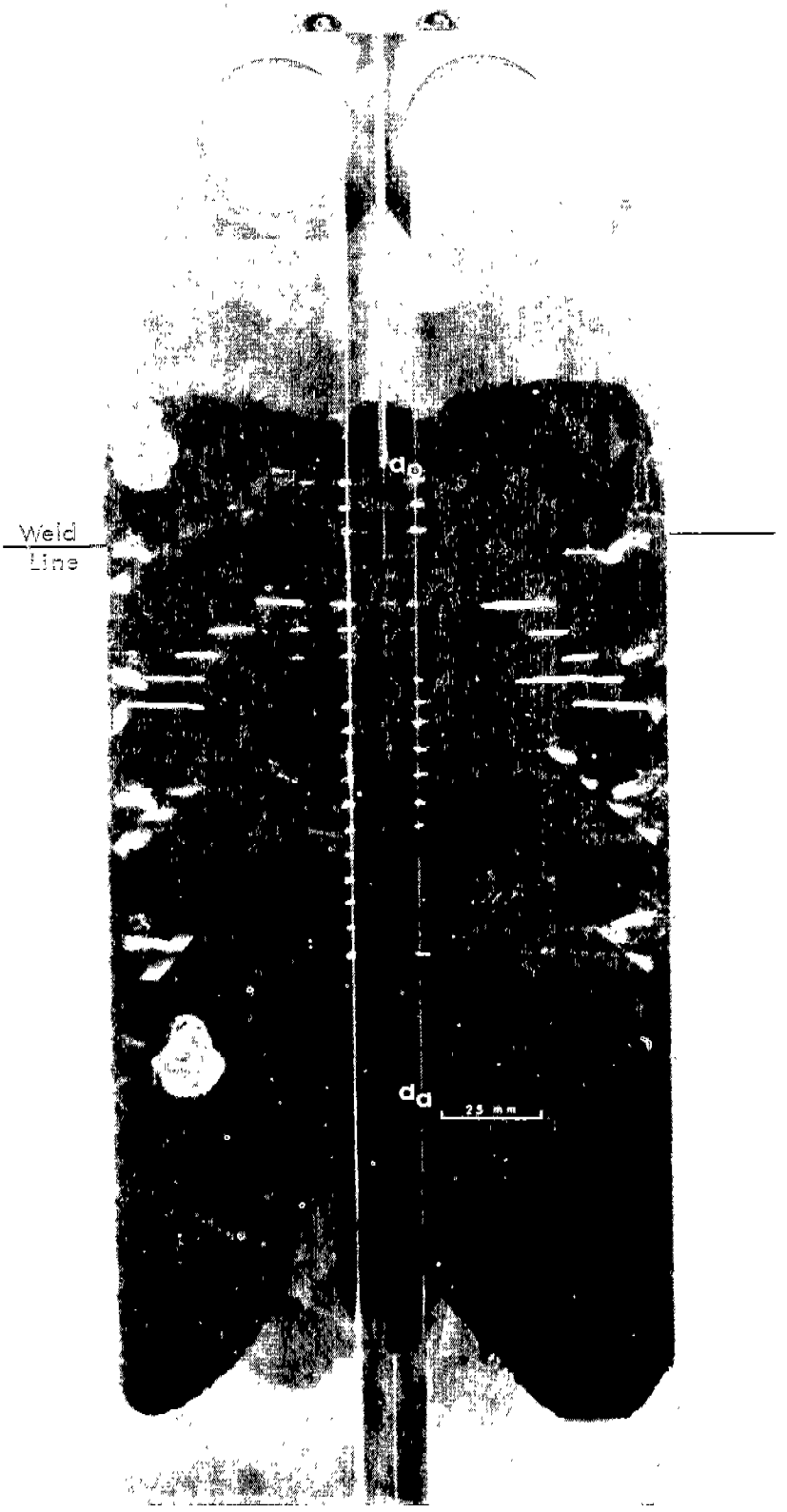

FIGURE 10B. FULLY SIDE-GROOVED SPECIMEN

TABLE II. TEST SPECIMEN DESIGN CHARACTERISTICS

Specimen Numbers	Thickness (mm)	Type	Material	
			Starter Section	Test Section
A2-A4	12.7	Duplex	A517F	9% Ni
A5, A8	12.7	Duplex[a]	A517F	9% Ni
A6, A7	12.7	Duplex, Test Section Side Grooved	A517F	9% Ni
F1, F2, F4, F5	25.4	Duplex, Test Section Side Grooved	4340	ABS-C
F3, F6, F7, F8	25.4	Duplex, Fully Side Grooved	4340	ABS-C
G1-G3	25.4	Duplex, Test Section Side Grooved	4340	ABS-E
G4-G6	25.4	Duplex, Fully Side Grooved	4340	ABS-E
H1-H5	25.4	Duplex, Test Section Side Grooved	4340	ABS-EH
H6, H7	25.4	Duplex, Fully Side Grooved	4340	ABS-EH
VY10-13	12.7	Duplex	4340	A517F
VY23, VY28	25.4	Duplex	4340	A517F
VY26	25.4	Duplex, Test Section Side Grooved	4340	A517F
VYV1-VYV-6	12.7	Arrestor	4340	A517F[b]
Y2-Y5	12.7	Ordinary	--	A517F
Z1-Z4	12.7	Ordinary	--	A517F

(a) Contained side groove extending 16mm into test section.
(b) Arrestor strip.

Dynamic toughness values were obtained from the analysis of Kanninen.[22,23] A feature of this analysis is that the crack velocity is determined by the ratio of K_D to K_Q and does not depend sensitively on the shape of the K_D vs velocity curve. Figure 11 shows the relation among these quantities for the dimensions adopted for all of the specimens (except a few of the ordinary A517F tests). Given the steady-state velocity and K_Q, which is the effective static stress intensity at the onset of rapid crack propagation, K_D can be determined from the graph. For duplex specimens, individual K_D values for the separate sections can be determined from K_Q and the velocity measured in each section.

RESULTS

A517F

Table 3 lists the experimental results, while the data are plotted in Figures 12-14. K_D values are taken from the data of Barsom and Rolfe [10]. Although there are insufficient points to define the full K_D versus velocity curve at any one temperature, several trends are clear. Chief among these is the increasingly higher values of dynamic toughness at the higher temperatures. This effect may be due partially to the loss of constraint as the temperature is raised and, consequently, as the yield stress is lowered. Some loss of constraint is evident from the thickness effect at -78°C and constraint is probably lost at the higher temperatures. There is some added uncertainty to the results at the highest temperatures (-35 to -54°C). In three of these specimens the crack arrested within the arrestor strip. The velocities plotted appear to be steady-state, but might actually represent deceleration. Therefore, the plotted velocities might be underestimates, possibly by as much as 200 m/s. At the same time, K_D is calculated from the velocity via Figure 5c of Reference [17]. If the actual velocity is 200 m/s higher than the reported value, the dynamic fracture toughness would be 10-20% lower. The fourth point of this series exhibited a much higher velocity and lower toughness than the other three for reasons that are not clear.

The data at -196°C are shown on an expanded scale in Figure 13. The zero velocity value is K_{Ic}. Our value for reinitiation from a sharp crack agrees with the values reported by Barsom and Rolfe [10] and by Tetelman, et al [24]. The parabolic curve has the equation

$$K_D = K_{Ic} \left\{ 1 - 3.8 \left(\frac{v}{c_o} \right) + 38 \left(\frac{v}{c_o} \right)^2 \right\} \qquad (6)$$

where c_o is the bar wave speed. Equation 6 is of the form generally accepted for cleavage failure: with increasing velocity K_D first decreases, passes through a minimum and then begins to increase rapidly.[25] The coefficients of Equation 6 were determined from the data where crack velocities were measured. Note also that this equation is identical in form to the rate-dependent material of Kanninen's [19] calculation with the minimum value of $K_D = 0.91\ K_{Ic}$ occurring at a velocity of $0.05\ c_o$.

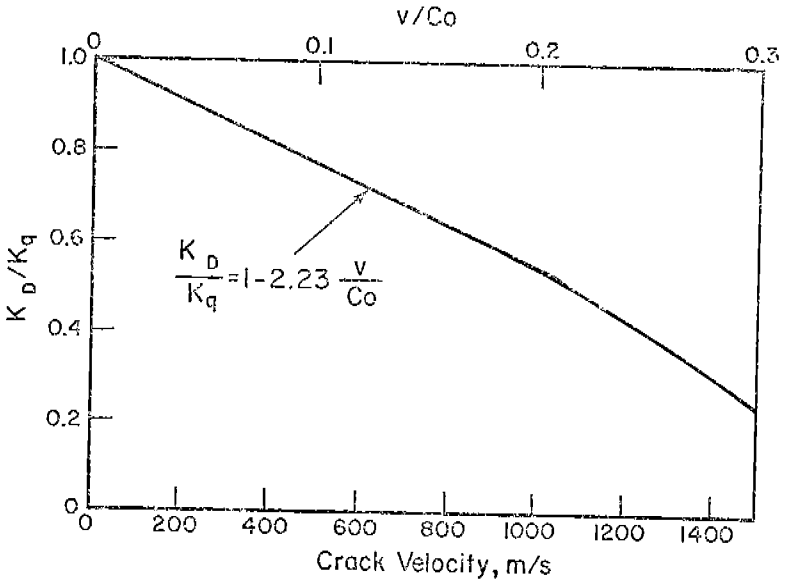

FIGURE 11.

RELATION BETWEEN CRACK VELOCITY AND DYNAMIC FRACTURE TOUGHNESS FOR THE DOUBLE-CANTILEVER-BEAM SPECIMEN

Dimensions used in the calculation are:

overall length = 400 mm, width = 140 mm, thickness = 12.7, initial crack length (measured from center line of pin holes) = 84 mm, diameter of pin holes = 38 mm.

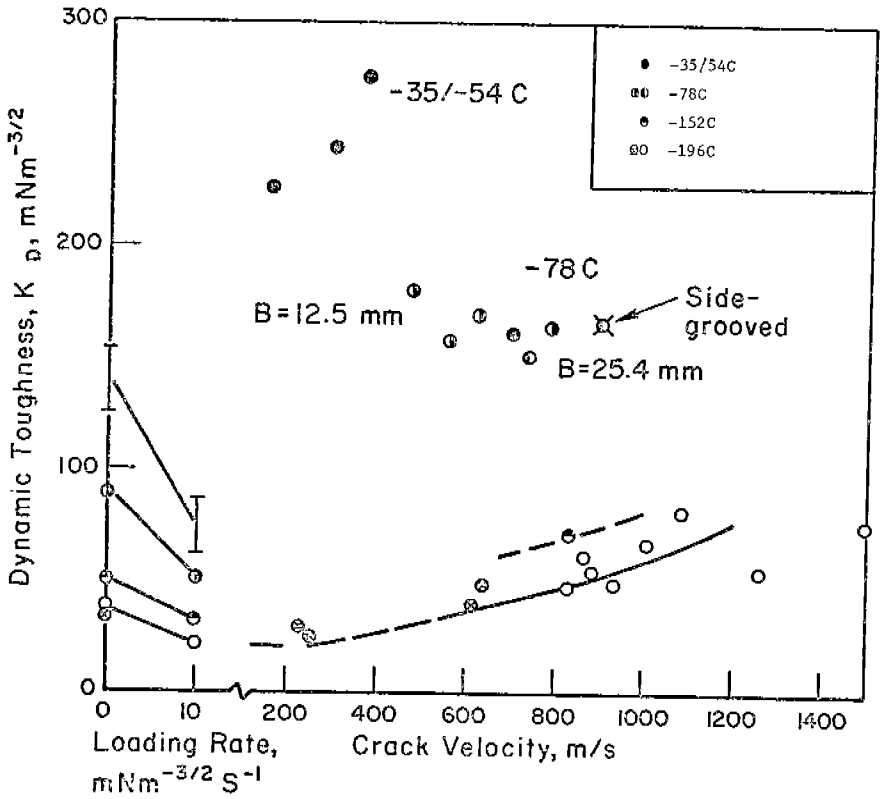

FIGURE 12. IMPACT RATE AND CRACK VELOCITY DEPENDENCE OF DYNAMIC TOUGHNESS OF A517F STEEL OVER A RANGE OF TEMPERATURES. Points marked @ represent calculated velocities. All others were measured. K_D data from Barsom and Rolfe [11]

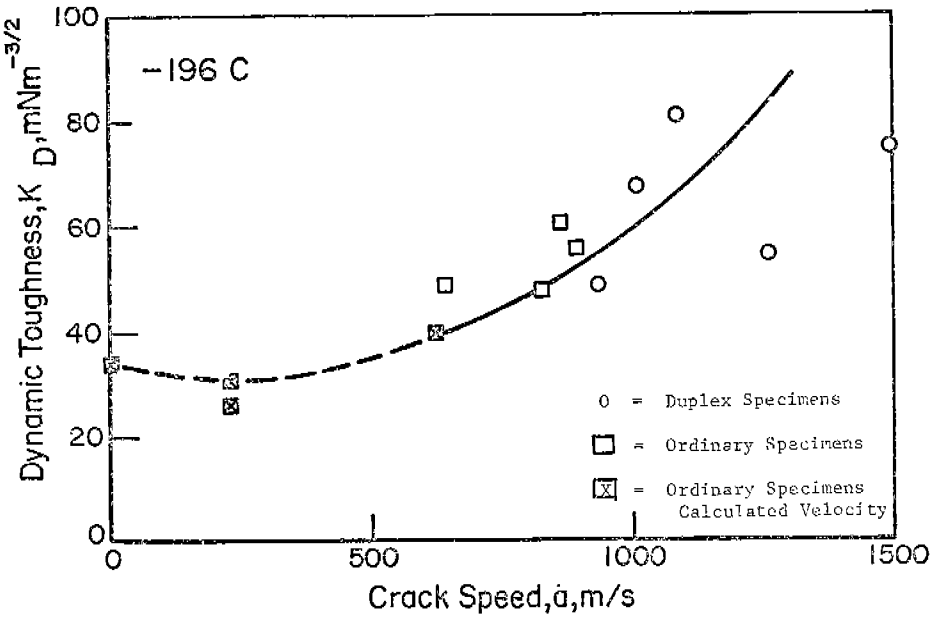

FIGURE 13. EFFECT OF CRACK VELOCITY ON DYNAMIC TOUGHNESS OF A517F STEEL AT -196°C

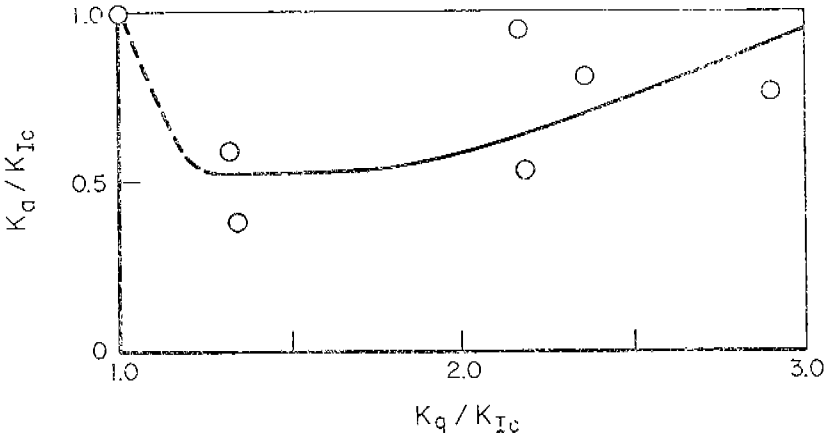

FIGURE 14. RELATION BETWEEN STRESS INTENSITY AT CRACK ARREST AND STRESS INTENSITY AT THE ONSET OF RAPID CRACK PROPAGATION IN THE WEDGE-LOADED DCB SPECIMEN. A517F Steel Tested at -196°C.

TABLE III. CRACK PROPAGATION AND ARREST DATA FOR A517F STEEL

Specimen No.	Temperature (°C)	Crack Velocity (m/s)	Dynamic Toughness, K_D $MNm^{-3/2}$	Stress Intensity at Arrest, K_a, $MNm^{-3/2}$
		Duplex Specimens		
VYV-1	-48/-50[a]	700	161	--
-3	-52/-54[a]	155	225	--
-5	-35/-44[a]	370	276	207
-6	-44/-48[a]	300	242	217
VY-10	-78	475	180	114
-12	-78	560	159	102
-13	-78	625	170	68
-23[b]	-78	740	159	∿73[d]
-26	-78	900	167	--[d]
-28	-78	780	164	∿78[d]
A-2	-152	830	73	--
-3	-196	940	49	--
-4	-196	1010	68	--
-5	-196	1500	75	--
-6	-196	1090	81	--
-8	-196	∿1260	54	--
		Ordinary Specimens		
Z-1	-196	0[c]	34	34
-2	-196	(230)[c]	31	20
-3	-196	(240)[c]	26	13
-4	-196	(620)[c]	40	18
Y-2	-196	640	49	33[d]
-5	-196	870	61	--[d]
-3	-196	830	48	28[d]
-4	-196	890	56	27[d]

(a) Temperature variation over the crack path.
(b) Side-grooved in test section.
(c) Estimated from relation between K_Q and crack velocity.
(d) Crack ran to one side.

The points on Figure 12 represent two different size samples with the velocity measurements having been made on larger samples and the velocity estimates on smaller samples. In particular the ratio of initial crack length to beam height (a_o/h) was > 1 and < 1, respectively. While it was not possible to locate the toughness minimum precisely using the present data, there is no reason to modify the view [25] that it occurs at a few hundred m/s at low temperatures.

The crack arrest data at -196°C, shown in Figure 14, are of interest for several reasons. In the first place, K_a is clearly not constant but a function of the initial conditions as expressed by K_Q (the stress intensity at crack extension) and of the material as expressed by K_{Ic}. Secondly, the K_a values associated with rapidly moving cracks are larger than for more slowly moving cracks. This is in accord with Kanazawa's [26] analysis of his data since the velocities in his large plates are larger than in the small plates. This result arises partially from the higher energies needed to sustain more rapid cracks. Indeed, if the material were rate independent K_a would decrease with increasing velocity.[19]

9% Ni Steel (A553)

Most of the experiments were performed at -196°C, the results for this temperature being given in Table 4 and Figure 16. The toughness values associated with rapid crack propagation appear to be not too much higher than those associated with extension from an initially sharp crack. That the resistance to fast fracture in Mode I is not extremely high is illustrated by Specimen 7 which broke completely in two. The side grooves were required to provide crack penetration into the A553. In specimens without side grooves the crack arrested upon encountering the test section. Two of the points listed in the Table are not plotted on the graph. One of these (Specimen 6) represents a measurement deduced from crack velocity data where the trace was quite poor and prevented an accurate value. The other inaccurate point was calculated using Equation A-4 for a sample (Specimen 8) where the crack penetration into the test section was small, resulting in a large relative error. Both of these values were much higher than the comparison measurements on the same specimen. The points plotted on Figure 16 may well be conservative for this reason as well as because of the use of side grooves.

While comparison with data from other investigators may not be meaningful because of the extreme sensitivity of toughness to heat treatment, it is interesting to note that Vishnevsky and Steigerwald [11] report K_c values for crack initiation ≈ 120 MNm$^{-3/2}$ for a heat treatment reasonably close to the one used in this investigation. Our datum point for the very low velocity of 45 m/s is close to this value.

Experiments at higher temperatures were only partially successful. As discussed in Appendix A it is possible to set some bounds on the dynamic toughness at -152 and -164°C. It appears that K_D is not very much larger at these temperatures than at -196°C, a trend also apparent in the data for K_Q values for crack initiation from a sharp notch.[12,13]

Scanning electron microscopy (Figure 17a) revealed that the micromechanism of fracture was dimpled rupture. In addition, a number of sharp ridges are observed. On other parts of the surface, the ridges are replaced by valleys. While the cause of these ridges and valleys was not investigated in detail, they are probably related to inhomogeneities in the microstructure resembling banding and shown in Figure 17b.

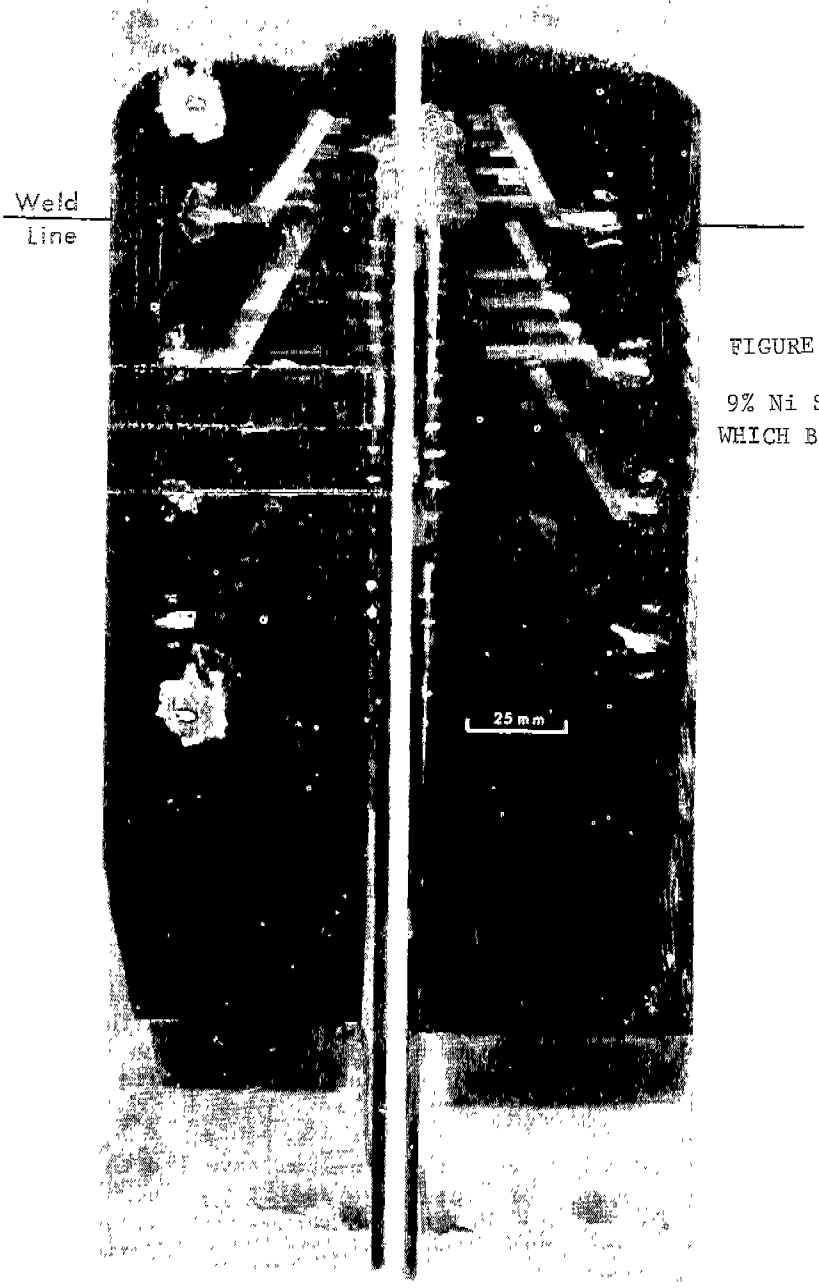

FIGURE 15.

9% Ni STEEL SPECIMEN A-7
WHICH BROKE IN TWO AT -162°C

TABLE IV- DYNAMIC FRACTURE IN DUPLEX SPECIMENS CONSISTING OF A517F AND 9% Ni STEELS

(a) Crack Initiation and Arrest Data

Specimen No.	Temp. (C)	Root Radius of Starter Notch (mm)	Crack Penetration Into Test Section (mm)	Stress Intensity ($MNm^{-3/2}$) Crack Initiation,	Crack Arrest, Ka
A-3	-196	0.14	0	98	> 73
A-4	-196	0.56	0	142	>101
A-6[a]	-196	0.55	136	248[d]	59
A-8[b]	-196	0.81	7.4[b]	118	73
A-5[b]	-196	0.93	16.3	259	111
A-2	-152	0.25	2.4	134	95
A-7[a]	-164	0.57	(c)	395[d]	(c)

(a) Side-grooved.

(b) Side-groove only extended 16 mm into the test section.

(c) Specimen broke completely in two.

(d) Based on specimen width at side grooves.

TABLE IV. DYNAMIC FRACTURE IN DUPLEX SPECIMENS CONSISTING OF A517F AND 9% Ni STEELS

(b) Crack Propagation Data

Specimen No.	Temp. (C)	Stress Intensity and Fracture Toughness ($MNm^{-3/2}$)			Crack Velocity (m/s)	
		Kq	K_D (A517)	K_D (A553)	A517	A553
A-3	-196	98	49[c]	>98[a]	940	(a)
A-4	-196	142	68[c]	>142[a]	1010	(a)
A-6	-196	248[f]	81[c]	130[b], 220[c],[d]	1090	~300
A-8	-196	118	54[c]	181[b],[d], 116[c]	~1260	45
A-5	-196	259	75[c]	<162[b], 130[c]	1500	1070
A-2	-152	134	73[c]	>134	830	(a)
A-7	-164	395[f]	--	≤160	--	(e)

(a) Did not penetrate test section.

(b) Based on crack arrest.

(c) Based on crack velocity.

(d) Value subject to large errors, see text.

(e) Specimen completely broke in two.

(f) Based on specimen width at side grooves.

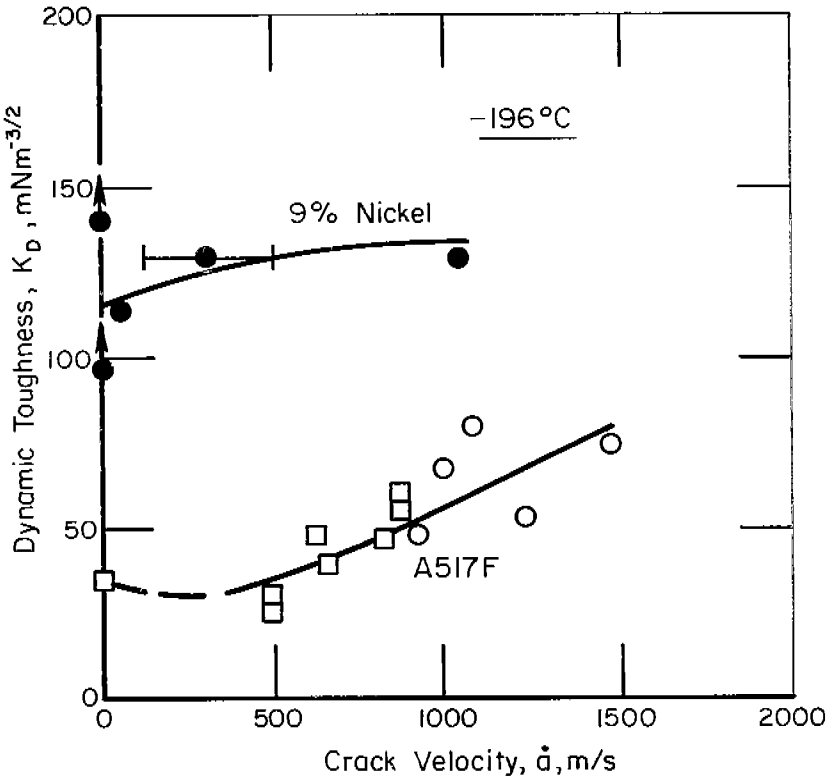

FIGURE 16. DYNAMIC FRACTURE TOUGHNESS OF 9% Ni STEEL COMPARED TO THAT OF ASTM-A517F

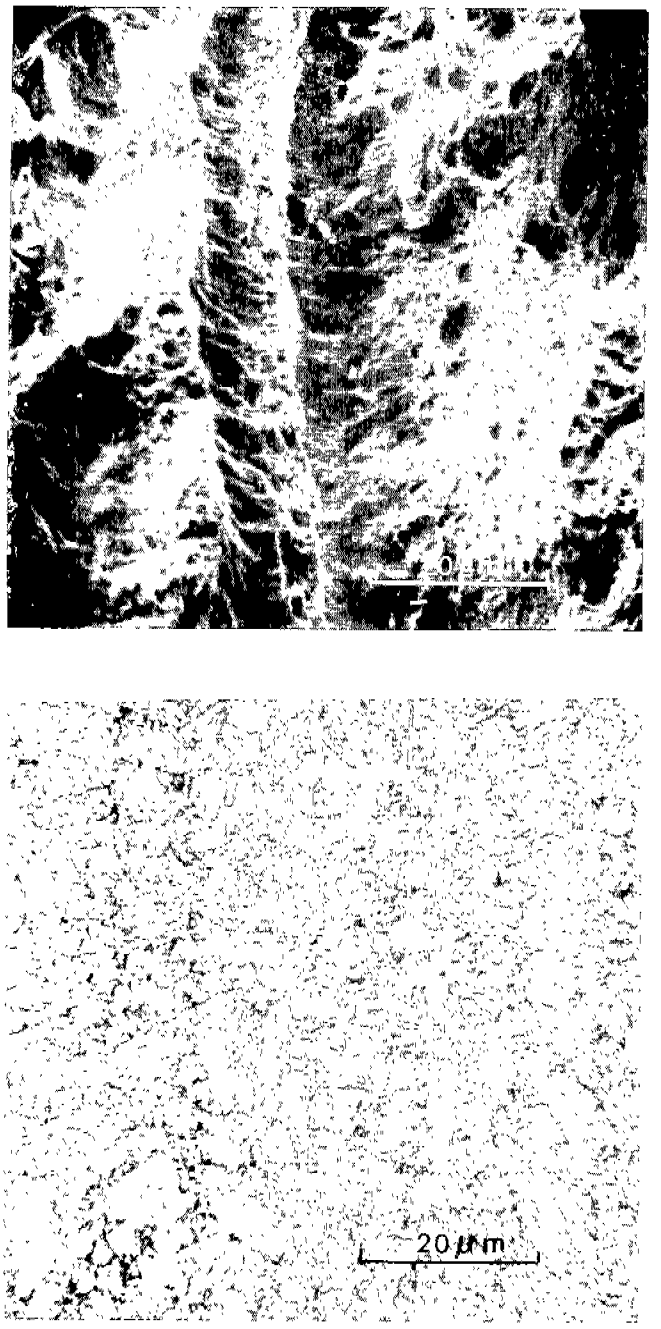

FIGURE 17. METALLOGRAPHIC OBSERVATIONS OF A553 (9% Ni) STEEL.

In both pictures the horizontal direction is through the thickness.

(a) Fractograph illustrating dimpled rupture and ridges.

(b) Light migrograph normal to the fracture surface illustrating "banding".

The dynamic toughness of 9% Ni steel contrasts sharply with that of A517F as shown in Figure 16. In turn, the behavior of A517F is characteristic of steels tested below their ductile-brittle transition temperatures.[25] While the velocity dependence of the 9% Ni steel is not particularly well defined, the curve appears to be somewhat flatter than those for higher strength steels which fail by dimpled rupture when tested at room temperature.[27] It would appear that the cleavage and dimple rupture mechanisms result in different forms of the toughness/velocity curve.

Because of the presence of side grooves, the values cited here are for fast fracture characteristics of thick sections and only for one particular heat treatment. The Charpy data indicate that the heat treatment used on our experimental material produced the lowest toughness levels of any within ASTM-A553. It is reasonable to assume that the K_D values for this steel in the quenched and tempered condition can be raised to levels considerably above 130 $MNm^{-3/2}$ even in the presence of side grooves.

ABS-C, -E, and -EH Steels

Complete experimental results are listed in Table 5. For all three steels, the temperature range spans NDT and extends over ∿100°C. Crack velocities range from 380-1120 m/s, whereas the limiting speed is estimated to be ∿2,000 m/s. With three exceptions K_D values exceed 100 $MNm^{-3/2}$, whereas K_{Id}, the energy associated with crack initiation by impact, is reported to be ≤50 $MNm^{-3/2}$.[7,28] Thus, the energy absorbed by a rapidly propagating crack appears to be in excess of that required to initiate a crack by dynamic loading.

Figure 18 shows the temperature dependence of K_D for each of the three steels along with the dynamic tear energies for the same plates measured by Hawthorne and Loss.[5] While there is quite a bit of scatter, it is clear that NDT marks an upturn in the toughness versus temperature curve. Also Figure 18 suggests that the steels can be best compared by referring to NDT as a standard. This is done in Figure 19. Only those specimens for which velocity traces are available have been included, since toughness depends on crack velocity as well as test temperature. Note particularly that the data are ordered with respect to crack velocity, with the lower velocities systematically associated with higher toughness. In particular, the toughness associated with the highest velocities appears to be temperature-independent and about equal to 100 $MNm^{-3/2}$ over a 60°C span in temperature. The values are also seen to be considerably higher than the lower bond values which have been suggested based on K_{Ic} and K_D measurements.[9,29]

The velocity dependence of toughness at NDT, deduced from Figure 19, is shown in Figure 20. Also shown in Figure 20 are data on A517F steel,[21] as well as K_D values for C steel and A517F.[7] A steep dependence of toughness on velocity, common to all four steels, is revealed. In particular, the behavior appears to fit the descending segment of the idealized material B curve (Figure 18). A moot point remains as to whether still lower values of K_D would be observed if higher velocities were achieved and whether K_D approximates the minimum in the toughness versus velocity curve.

TABLE V. CRACK PROPAGATION AND ARREST BEHAVIOR OF SHIP-HULL STEEL

a. Crack Initiation and Arrest Data

Specimen No.	Temperature (°C)	Root Radius of Starter Notch (mm)	Crack Penetration into Test Section (mm)	Stress Intensity ($MNm^{-3/2}$)	
				Crack Initiation, K_Q	Crack Arrest, K_a
			C Steel (NDT = - 12°C)		
F-2	24	0.65	61.0	239	98-143
F-1	9	0.66	73.7	251	93-160
F-5(a)	-12	0.56	(b)	264	-
F-6(a)	-12	0.58	104.9	211	58-90
F-7(a)	-31	0.57	(b)	174	-
F-3(a)	-50	0.57	(b)	158	-
F-8(a)	-53	0.56	119.9	145	35-90
F-4	-80	0.58	(b)	239	-
			E Steel (NDT = - 23°C)		
G-2	8	0.62	156.4	228	49-129
G-1	-12	0.69	15.2	224	139-287
G-5(a)	-17	0.56	(b)	190	-
G-3	-40	0.56	(b)	246	-
G-4(a)	-60	0.58	>61.0(c)	168	69-164
G-6(a)	-80	0.61	(b)	171	-
			EH Steel (NDT = - 51°C)		
H-3	24	0.56	31.8	236	128-225
H-7(a)	0	0.57	21.8	189	103-149
H-1	-17	0.67	55.9	284	121-225
H-4	-17	0.56	62.5	280	108-212
H-5	-54	0.58	(b)	224	-
H-6(a)	-94	0.56	(b)	191	-

(a) Fully side-grooved.
(b) Specimen broke completely in two.
(c) Crack ran out of side groove.

TABLE V. CRACK PROPAGATION AND ARREST BEHAVIOR OF SHIP-HULL STEEL

b. Crack Propagation Data

Specimen No.	Temperature °C	Test Temperature Minus NDT (°C)	Crack Velocity (m/s)	Stress Intensity and Fracture Toughness ($MNm^{-3/2}$)	
				Stress Intensity at Crack Initiation, K_Q	Dynamic Toughness K_D
		C Steel (NDT = - 12°C)			
F-2	24	36	550	239	182
F-1	9	21	540	251	193
F-5	-12	0	890	264	101
F-6(a)	-12	0	500	211	164
F-7(a)	-31	-19	500	174	135
F-3(a)	-50	-38	-	158	<63(b)
F-8(a)	-53	-41	-	145	56(c)
F-4	-80	-68	-	239	<102(b)
		E Steel (NDT = - 23°C)			
G-2	8	31	-	228	180(c)
G-1	-12	11	380	224	190
G-5(a)	-17	6	1120	190	90
G-3	-40	-17	1070	246	115
G-4(a)	-60	-37	1020	168	90
G-6(a)	-80	-57	820	171	109
		EH Steel (NDT = - 51°C)			
H-3	24	75	800	236	165
H-7(a)	0	51	-	189	135(c)
H-1	-17	34	380	284	235
H-4	-17	34	450	280	225
H-5	-54	- 3	1020	224	114
H-6(a)	-94	-43	920	191	113

(a) Fully side-grooved.
(b) Estimated from $K_Q/2.5 = K_D$.
(c) Based on arrest length.

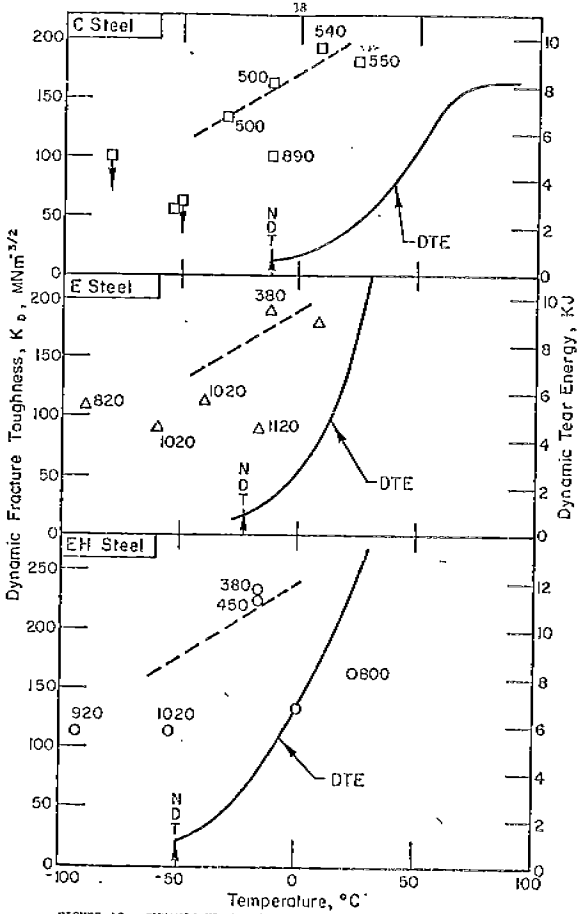

FIGURE 18. DYNAMIC FRACTURE TOUGHNESS AND DYNAMIC TEAR ENERGY VALUES FOR THREE SHIP-PLATE STEELS
Dynamic tear energy from Reference [5]
(The numbers adjacent to the points are crack velocities in m/s).

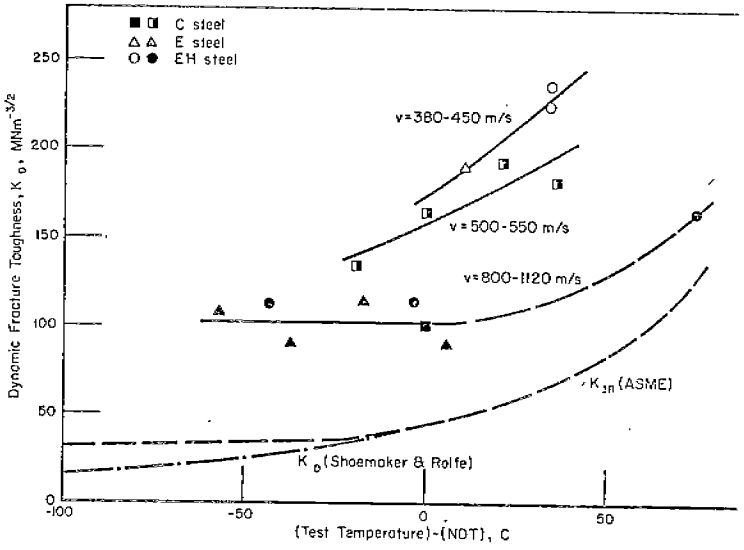

FIGURE 19. DYNAMIC TOUGHNESS AS A FUNCTION OF CRACK SPEED AND TEMPERATURE (referred to NDT). K_D data from Reference 7, K_{ID} data from Reference [29].

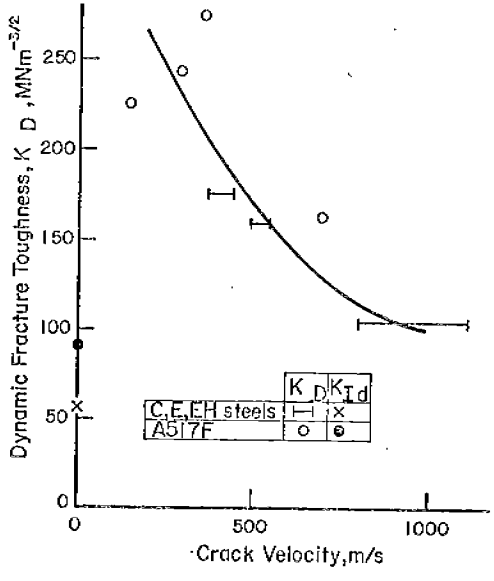

FIGURE 20. RELATION BETWEEN CRACK VELOCITY AND DYNAMIC TOUGHNESS FOR STEELS TESTED NEAR NDT
Initiation Data from References 7 and 10.

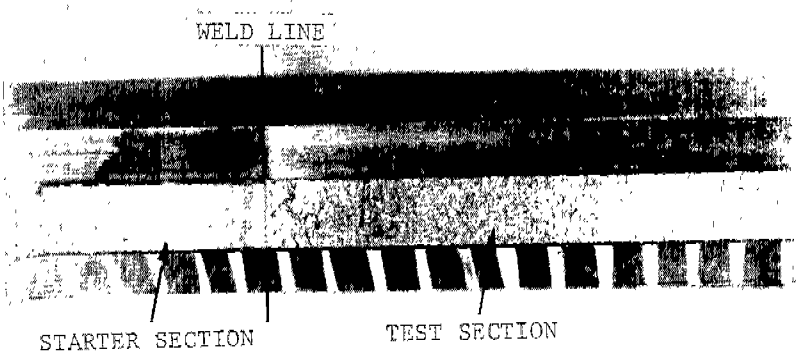

(a)

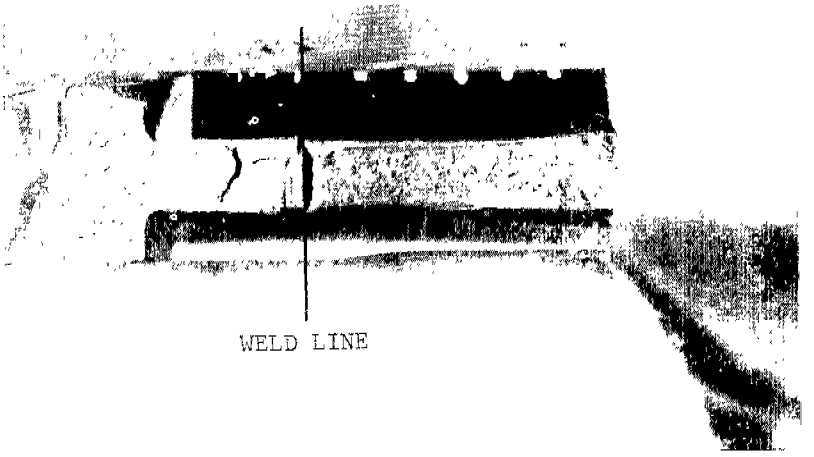

(b)

FIGURE 21. FRACTURE APPEARANCE OF SHIP-HULL STEELS

a. ABS-E tested at -17°C; crack velocity = 1120 m/s, K_D = 90 $MNm^{-3/2}$.

b. ABS-EH tested at 24°C; crack velocity = 800 m/s, K_D = 165 $MNm^{-3/2}$.

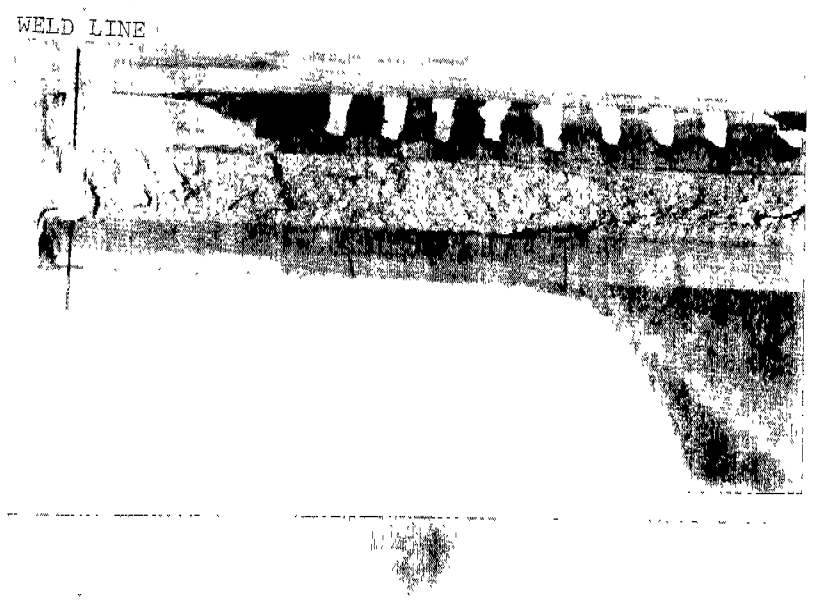

(c)

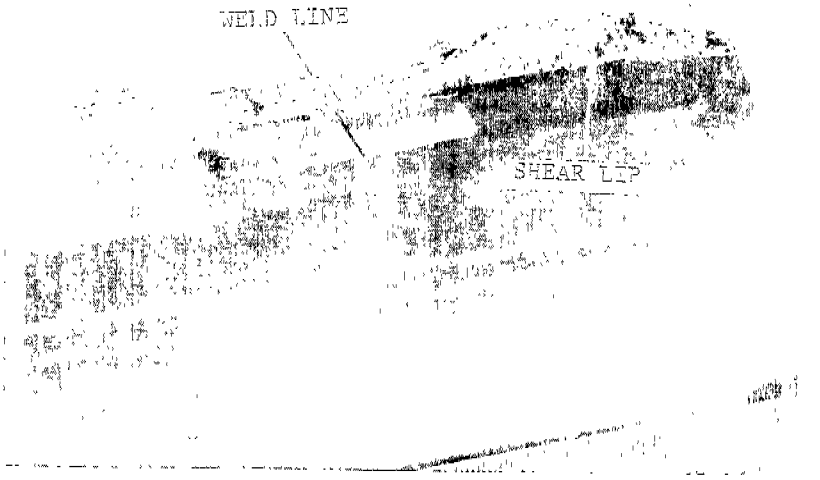

(d)

FIGURE 21. FRACTURE APPEARANCE OF SHIP-HULL STEELS (Continued)

(c) ABS-C tested at 9°C; crack velocity = 540 m/s, K_D = 193 $MNm^{-3/2}$.

(d) ABS-EH tested at -17°C; crack velocity = 450 m/s, K_D = 225 $MNm^{-3/2}$.

The fracture appearances of the different velocity regimes (and thus different toughness levels), are consistent with the velocity-sensitive behavior shown in Figure 20. Four different surface morphologies were noted as illustrated in Figure 21:

(a) Velocity $\simeq$ 1000 m/s, Temperatures $\leq$ NDT: Figure 21a shows a fracture surface which is quite flat and shiny, typical of a low-energy cleavage fracture.

(b) Velocity $\simeq$ 800 m/s, Temperature = NDT + 75°C: Figure 21b shows a fracture surface that is dull and flat. Only one specimen displayed this behavior.

(c) Velocity $\simeq$ 500 m/s, Temperatures Between NDT -20°C and NDT + 50°C: The fracture surface illustrated in Figure 21c is flat but also contains large cleavage facets. The behavior was confined to C steel.

(d) Velocity $\simeq$ 400 m/s, Temperatures > NDT: Three samples of Grades E and EH steel displayed the behavior shown in Figure 21d which was characterized by combined flat fracture and shear lip formation. The shear lip formed at the root of the side groove is parallel to the broad face of the test specimen. Thus it is a mirror image of the shear-lip formed in a flat-sided plate.

The stress intensity values at crack arrest tended to increase with increasing temperature. All of the values obtained are plotted in Figure 22, again using NDT as a reference temperature to provide a common basis for comparison. Two values of K_a are plotted, a lower limit corresponding to the displacement value at crack extension and an upper limit corresponding to the larger displacement attained after the machine has provided additional energy to the specimen. Note particularly that the values of K_a within the narrow temperature range of NDT + 30°C to NDT + 36°C vary by a factor of two. This observation is not surprising, since K_a is not a material constant but is determined by the history of energy absorption during crack propagation. Also indicated on Figure 21 is the K_D versus temperature curve for crack initiation in C steel, and the K_{IR} curve adopted by ASME [29] on the basis of tests on A533B. K_{IR} is a lower bound for all reported toughness measurements for this latter steel and contains some K_{Ia} values. These two latter curves are a rough lower limit for the present data, but tend to underestimate the results seriously for most specimens.

DISCUSSION OF RESULTS

Taken together, the experimental results define a consistent picture of the fracture process and provide added support for the energy balance approach.

Previous results [18,27] have shown that crack propagation associated with the ductile dimple mechanism results in a monotonically rising K_D vs crack velocity curve. The curve for the 9% Ni steel (Figure 16) is of the same shape but somewhat flatter than that of the high-strength steels studied earlier. [18,27]

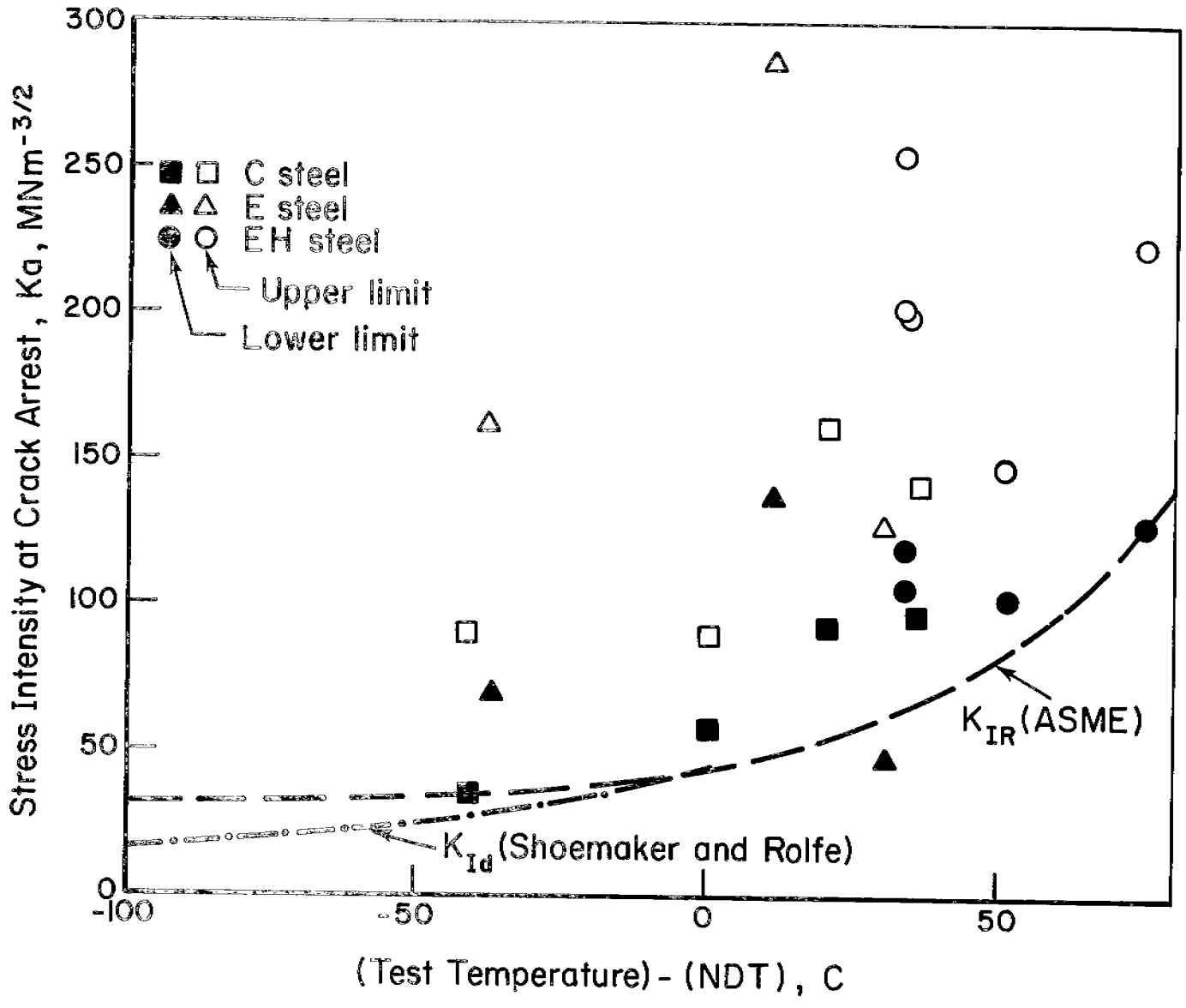

FIGURE 22. CRACK ARREST DATA FOR THREE SHIP-HULL STEELS

The 9% Ni steel displays a much higher resistance to fast fracture at -162°C and -196°C than ordinary ship grades (i.e. ABS-C, -E and -EH) tested at the same temperatures (See Figure 2). But, it is also important to note that the K_D values obtained for the 9% Ni steel at -162°C and -196°C are comparable to those measured for the ordinary grades in the vicinity of the NDT, where the resistance to fast fracture is acknowledged to be marginal. The test piece illustrated in Figure 15 which broke in two, at a velocity estimated to be on the order of 1000 m/s at -162°C is evidence of the normal nature of the toughness. In other words, the fast fracture resistance of the material in the form of present, side grooved laboratory test peices is not large enough at -162°C and -196°C to preclude fast running fractures in large structures. However, the qualifications contained in the two underlined words must also be weighed. First, the side grooves used in the present experiments tend to inhibit surface shear and shear lip formation which can consume twice as much energy as equivalent amounts of that fracture. Consequently, the present results, while valid for relatively thick plates, may understate the toughness of the 12.7mm thick 9% Ni steel. Additional studies of test pieces without side grooves are needed to obtain a better definition of K_D are needed. Secondly, there should be scope to improve the fast fracture resistance via heat treatment as discussed earlier.

The curve for A517F tested far below NDT where the cleavage mechanism predominates appears to exhibit a toughness minimum at velocities on the order of a few hundred m/s, in accord with the picture of Eftis and Krafft.[25] The results available from the literature [25,28,30] and some preliminary results from the present study, as shown in Figure 23, support the existence of the minimum although its precise depth and the corresponding velocity are poorly defined.

Any decrease in toughness with increasing velocity will result in an instability in that progressively higher velocities absorb progressively less energy. The data for the ABS steels at NDT reported here suggests that this instability persists even into the transition range. The initial decrease in the toughness/velocity curve may be connected with the competition between yielding and cleavage. As the crack travels more rapidly, yielding is inhibited and less energy is dissipated by plastic flow. As the temperature is raised above NDT, the energy increases and it becomes progressively more difficult to generate a fast moving crack in the ship steels. The experiments were not extended to a sufficiently high temperature to determine the upper plateau in toughness.

The minimum value of the K_D vs. velocity curve was not determined. From Figure 19, it would appear the $K_{D(min)} \leq 105$ $MNm^{-3/2}$ at NDT. At the same time K_a (the stress intensity at crack arrest), appears to be ≥ 80 $MNm^{-3/2}$ at NDT. Calculations by Kanninen [19] for the double cantilever beam geometry suggest that $K_a \sim (0.6\text{-}1.1)\ K_{D(min)}$ with a typical value of $0.8\ K_{D(min)}$. Thus one can estimate $K_{D(min)} \sim 100$ $MNm^{-3/2}$, which is close to the lowest values observed herein. Since K_D appears to be sensibly independent of velocity over a range of 800-1120 m/s, it might be assumed that the minimum has been located. However, more extensive data are needed.

A quantity which has been suggested as characterizing fast fracture resistance is K_{Id} the toughess associated with rapid crack initiation. Several authors [1,5,31-33] have estimated that K_{Id} at NDT is:

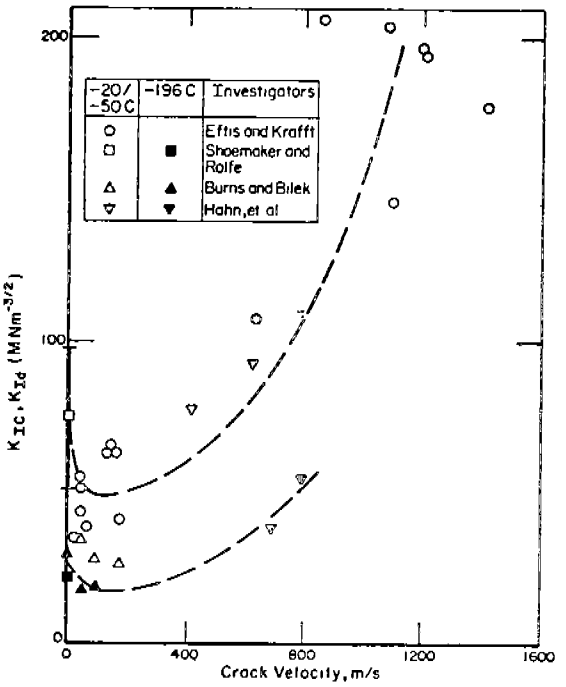

FIGURE 23. A SUMMARY OF DIRECT MEASUREMENTS OF THE DYNAMIC FRACTURE TOUGHNESS OF PLAIN CARBON STEELS BELOW NDT
Data from References [25,28,30]

$$\frac{K_{Id}}{\sigma_{Yd}} = (0.06\text{-}0.12)\ m^{1/2} \qquad (7)$$

where σ_{Yd} is the dynamic yield stress, which can be approximated by adding 210 MNm^{-2} to the static room temperature yield stress, to compensate for rate effects and for the temperature difference between ambient and NDT.

The minimum K_D values obtained in this laboratory at temperatures on the order of NDT are summarized in Table 6. Note that these lowest values are roughly twice as large as K_d determined from Equation 7. Accordingly, it appears that K_d, as well as K_a, underestimates the fast fracture resistance of the steel. However, the values cited in Table 6 are not necessarily the minimum values of K_D with respect to velocity, $K_{D,min}$, which may be closer to the values of K_d. This point requires further investigation.

TABLE VI – LOWEST MEASURED VALUES OF K_D FOR STEELS AT TEMPERATURES CLOSE TO NDT

Steel	NDT (°C)	Test Temperature (°C)	K_D/σ_{Yd} ($m^{1/2}$)	Reference
A517F	-40	-50	0.16	This work
A533B	-29	-18	0.17	[35]
ABS-C	-12	-12	0.21	This work
ABS-E	-23	-17	0.18	This work
ABS-EH	-51	-54	0.19	This work

It has also been suggested [7,34] that NDT is on the order of the temperature at which plane strain breaks down for a 25 mm thick specimen. To promote flat fracture, and to inhibit shear lip formation, the specimens used in the current investigation were deeply side grooved. Experiments on A517F at NDT -40°C and on 4340 [39] have suggested that side-grooving does not affect K_D in the absence of shear lips, but this point needs to be investigated more systematically. However, since shear-lip formation is inhibited by side-grooves, it is believed that the values reported here are either representative or conservative with regard to full-thickness behavior.

Dynamic tear energy is yet another measure of fast fracture resistance. Qualitatively, the variation of dynamic fracture toughness with temperature resembles the dynamic tear energy behavior (Figure 18). However, there are important quantitative differences between the two experiments. In the dynamic tear test, the loading conditions are not simple, the crack velocity is not necessarily constant, shear lip formation is not inhibited, and the kinetic energy contribution is not accounted for. For these reasons one would not expect a one-to-one correspondence between the two test procedures.

The strong dependence of toughness on crack velocity at NDT (Figure 20) illustrates one of the difficulties in interpreting energy absorption measurements such as are obtained via the dynamic tear test. Since the crack velocity history of the latter test is unknown, it is not clear what velocity or velocities the reported energies refer to. More seriously, it is not clear at what velocity a crack in a ship will propagate and what is the appropriate energy. The observation in this study that rapid cleavage fracture can occur at 10°C or more above NDT is borne out by the record of an actual failure within the past few years.[6]

The values of the stress intensity at crack arrest are very scattered (Figures 15 and 22). This observation is consistent with the energy balance approach.[23] In Appendix B this approach is used to estimate the largest tolerable size of embrittled region, i.e., the largest brittle region that the base plate can contain and still arrest a rapidly moving crack at NDT. The resulting equation is:

$$2a_e \approx \frac{1}{\pi} \left(\frac{K_D}{\sigma}\right)^2 \qquad (8)$$

where $2a_e$ is the width of the embrittled region and σ is the applied stress. In Appendix B typical values are inserted into eq. (8) and $2a_e$ is found to be $\approx$ 140mm (5-1/2"). This means that a flaw transverse to a weld line which becomes an unstable crack will be arrested by the base plate. While this calculation is admittedly crude, it gives an indication of the potential power of the methodology described in this report. In particular, the calculations in Appendix B show that the largest tolerable flaw size is a small multiple of the parameter, $(K_D/\sigma_{Yd})^2$, cited in Table 6. Accordingly significant benefits can be anticipated by defining composition and processing changes which increase K_D. The present research suggests that the K_D levels at NDT may not be susceptible to significant improvement in conventional ship steels. However, scope exists for reducing NDT so that it is well below service temperatures as suggested by Rolfe, et al [1].

CONCLUSIONS

(1) Rapid crack propagation and crack arrest in a variety of structural steels are governed by an energy balance approach.

(2) The controlling material property for propagation and arrest is the dynamic fracture toughness, K_D. Experiments reveal that K_D depends on fracture mechanism and crack velocity. There is also a temperature dependence of K_D within the cleavage crack propagation range. For the steels studied here, the dynamic fracture toughness is roughly twice the toughness associated with crack initiation by impact.

(3) The stress intensity at crack arrest after cleavage failure is not constant but varies in accord with the principle of conservation of energy.

(4) Dynamic fracture toughness values for a variety of ship-hull steels are similar to one another at their respective nil-ductility-temperatures (NDT).

ACKNOWLEDGEMENTS

The authors are greatful to the members of Advisory Group III of the Ship Research Committee for valuable guidence and discussions. Our colleagues at Battelle-Columbus provided important assistance, particularly C. R. Barnes, M. F. Kanninen, P. N. Mincer, and L. L. Wall.

REFERENCES

[1] S. T. Rolfe, D. M. Rhea, and B. O. Kuzmanovic, "Fracture-Control Guidelines for Welded Steel Ship Hulls", Ship Structure Committee Report SSC-244, 1974.

[2] G. T. Hahn, R. G. Hoagland, M. F. Kanninen and A. R. Rosenfield, "Crack Arrest in Steels", Engg. Fracture Mech., (in press).

[3] G. T. Hahn, R. G. Hoagland, M. F. Kanninen, A. R. Rosenfield, and R. Sejnoha, "Fast Fracture Resistance and Crack Arrest in Structural Steels", Ship Structure Report SSC-242, 1973.

[4] P. B. Crosley and E. J. Ripling, "Dynamic Fracture Toughness of A533 Steel", Trans. ASME, Vol. 91D, p. 525, 1969.

[5] J. R. Hawthorne, and F. J. Loss, "Fracture Toughness Characterization of Shipbuilding Steels", Ship Structure Committee Report SSC-248, 1974.

[6] U. S. Coast Guard, "Marine Casualty Report: Structural Failure of the Tank Barge I.O.S.3301 Involving the Motor Vessel Martha R. Ingram on 10 January 1972 Without Loss of Life", 1973.

[7] A. K. Shoemaker and S. T. Rolfe, "The Static and Dynamic Low-Temperature Crack-Toughness Performance of Seven Structural Steels", Engg. Fract. Mech., Vol. 2, p. 319, 1971.

[8] International Nickel Co., "9% Nickel Steel for Low Temperature Service", 1973.

[9] R. G. Hoagland, A. R. Rosenfield, and G. T. Hahn, "Mechanisms of Fast Fracture and Arrest in Steels", Met. Trans., Vol. 5, p. 123, 1972.

[10] Barsom, J. M. and Rolfe, S. T., "K_{Ic} Transition-Temperature Behavior of A517-F Steel", Engg. Fract. Mech., 2, 341, 1971.

[11] Vishnevsky, C., and Steigerwald, E. A., "Plane Strain Fracture Toughness of Some Cryogenic Materials at Room and Subzero Temperatures", ASTM STP 496, p. 3, 971.

[12] Bucci, R. J., Greene, B. N., and Paris, P. C., "Fatigue Crack Propagation and Fracture Toughness of 5 Ni and 9 Ni Steels", ASTM STP 536, p. 206, 1973.

[13] Tenge, P., and Solli, O., "9 Per Cent Nickel Steel in Large Spherical Tanks for Moss-Rosenberg 87600m^3 LNG-Carrier", European Shipbuilding, Vol. 21, p. 9, 1972.

[14] Duffy, A. R., and Eiber, R. J., "Fracture Behavior in Pipe Pressurized with LNG", Proc. Conference on Natural Gas Research and Technology (Inst. Gas Techn., Chicago), p. 11-1, 1971.

[15] Ooka, T., Mimura, H., Yano, S., Sugino, K., and Toizumi, T., "The Study on 9% Nickel Low Carbon Steels with Special Reference to the Relation Between the Precipitation Austenite and the Toughness of a 0.1%C 9% Nickel Steel", J. Japan Inst. Metals, Vol. 30, p. 442, 1966.

[16] Marschall, C. W., Hehemann, R. F., and Troiano, A. R., "The Characteristics of 9% Nickel Low Carbon Steel", Trans. ASM, Vol. 55, p. 135, 1962.

[17] Hahn, G. T., Hoagland, R. G., Kanninen, M. F., and Rosenfield, A. R., "The Characterization of Fracture Arrest in a Structural Steel", Pressure Vessel Technology, Part II, ASME, New York, 1973, 971.

[18] Hahn, G. T., Hoagland, R. G., Rosenfield, A. R., and Sejnoha, R., "Rapid Crack Propagation in a High Strength Steel", Met. Trans., 5, 475, 1974.

[19] Kanninen, M. F., "An Analysis of Dynamic Crack Propagation and Arrest for a Material Having a Crack Speed Dependent Fracture Toughness", Conference on the Prospects of Fracture Mechanics, Delft, Netherlands (in press).

[20] Hahn, G. T., Sarrati, M., and Rosenfield, A. R., "Plastic Zones in Fe-3Si Steel Double-Cantilever Beam Specimens", Intern. F. Fracture Mech., Vol. 7, p. 43, 1971.

[21] G. T. Hahn, R. G. Hoagland, and A. R. Rosenfield, "Temperatures Dependence of Rapid Crack Propagation and Arrest in A517F Steel", G. C. Sih, et al eds., Prospects of Fracture Mechanics, Noordhoff, Leyden (1974), p. 267.

[22] M. F. Kanninen, "A Dynamic Analysis of Unstable Crack Propagation and Arrest in the DCB Test Specimen", Int. J. Fracture, Vol. 10, p. 415, 1974.

[23] M. F. Kanninen, "An Analysis of Dynamic Crack Propagation and Arrest for a Material Having a Crack Speed Dependent Fracture Toughness", Conference on Prospects of Fracture Mechanics, Delft, Netherlands (in press).

[24] Tetelman, A. S., Wullaert, R. A., and Ireland, D., "The Use of the Precracked Charpy Specimen in Fracture Toughness Testing", Conf. on Practical Applications of Fracture Mechanics to Pressure Vessel Technology.

[25] Efis, J. and Krafft, J. M., "A Comparison of the Initiation with the Rapid Propagation of a Crack in a Mild Steel Plate", Trans. ASME, 87D, 257, 1964.

[26] Kanazawa, T., "Recent Studies on Brittle Crack Propagation in Japan", Dynamic Crack Propagation.

[27] Hahn, G. T., Hoagland, R. G., and Rosenfield, A. R., "Influence of Metallurgical Factors on Fast Fracture Energy Absorption Rates", submitted to Met. Trans.

[28] Shoemaker, A. K., and Rolfe, S. T., "Static and Dynamic Low-Temperature K_{Ic} Behavior of Steels", Trans. ASME, 91, Series D, 512, 1969.

[29] ASME Boiler and Pressure Vessel Code, Section III-Division 1, "Rules for Construction of Nuclear Power Plant Components", Subsection NA, "General Requirements", p. 491, 1974.

[30] Burns, S. J. and Bilek, Z. J., "The Dependence of the Fracture Toughness of Mild Steel on Temperature and Crack Velocity", Met. Trans., 4, 975, 1973.

[31] Irwin, G. R., Krafft, J. M., Paris, P. C., and Wells, A. A., "Basic Aspects of Crack Growth and Fracture", Naval Research Lab. Report 6598, 167.

[32] Server, W. L., and Tetelman, A. S., "The Use of Precracked Charpy Specimens to Determine Dynamic Fracture Toughness", Engg. Fract. Mech., Vol. 4, p. 367, 1972.

[33] Barsom, J. M., "The Development of AASHTO Fracture-Toughness Requirements for Bridge Steels", submitted to Engg. Fracture Mech.

[34] Robinson, J. N., and Tetelman, A. S., "The Critical Crack-Tip Opening Displacement and Microscopic and Macroscopic FractureCriteria for Metals", UCLA Report Eng-7360, 1973.

[35] Hahn, G. T., Hoagland, R. G., Kanninen, M. F., and Rosenfield, A. R., "Pilot Study of the Fracture Arrest Capabilities of A533B Steel", 9th National Symposium on Fracture Mechanics, Pittsburgh, Aug., 1975.

[36] Hoagland, R. G., and Rosenfield, A. R., "The Average Fracture Energy Accompanying Rapid Crack Propagation", Int. J. Fracture, Vol. 10, p. 299, 1974.

[37] Hoagland, R. G., Marschall, C. W., Rosenfield, A. R., Hollenberg, G., and Ruh, R., "Microstructural Factors Influencing Fracture Toughness of Hafnium Titanate", Mat. Sci. Engg., Vol. 15, 1974.

[38] Kanninen, M. F., "An Augmented Double Cantilever Beam Model for Studying Crack Propagation and Arrest", Int. J. Fracture Mech., Vol. 9, p. 83, 1973.

APPENDIX A

ANALYSIS OF THE SIDE-GROOVED DCB SPECIMEN

The energy extracted from a partially side-grooved DCB specimen such as shown in Figure 10, during crack propagation is found from:

$$\int_{a_o}^{a_r} dU = \int_{a_o}^{a_r} R'Bda \qquad \text{(A-1)}$$

where U is the stored elastic energy, a_r is the crack length at arrest, a_o is the crack length at initiation, B is the full thickness, and R' is the effective fracture energy given by:

$$\begin{aligned} R' &= R_s, \; a \leq a_1 \\ R' &= \frac{b}{B} R_T, \; a \geq a_1 \end{aligned} \qquad \text{(A-2)}$$

where R_S is the fracture energy of the starter section, R_T the fracture energy of the test section, b is the (reduced) thickness of the test section and a_1 is the crack length at the weld line between starter and test sections. Previous experiments, [17] confirmed by the present results, show that the crack propagates at a constant velocity in the starter section and at another constant velocity in the test section before it decelerates and arrests. Thus, it is reasonable to assume that there is a constant fracture energy in each of the sections.

To a good approximation: [9,36]

$$\int_{a_o}^{a_r} dU = (G_Q G_a)^{1/2} (a_r - a_o) \; (B) \qquad \text{(A-3)}$$

where GQ is the stress intensity at crack initiation and G_a is the stress intensity at crack arrest. Note that there are three sources of error in Equation A-3:

(1) It is an approximation of a more complex expression. However, within the range of normal specimen designs and distances of crack travel, it is an excellent approximation. [36]

(2) Within the context of Kanninen's beam-on-elastic-foundation model, [22,23] the foundation modulus should differ in the non-side-grooved and side-grooved regions of the specimen. This factor was not taken into account in the derivation of Equation A-3; the resulting error is not known but is believed to be quite small.

(3) There is a moment of inertia correction arising from the introduction of side grooves; [37] for typical DCB geometries used in these experiments, the correction is $\leq 1\%$.

Since the first two of these factors act in opposite directions, the overall error is believed to be well within the experimental uncertainity.

Combining Equations A-1 through A-3, rearranging terms, and expressing the results in terms of fracture toughness and stress intensity:

$$K_D(T) = \left(\frac{B}{b}\right)^{1/2} \left[\frac{(K_q K_a)(a_r - a_o) - K_D(S)(a_1 - a_o)^2}{a_r - a_1}\right]^{1/2} \qquad \text{(A-4)}$$

where $K_D(T)$ and $K_D(S)$ are the dynamic fracture toughness of the test and starter sections, respectively.

As before,[17] $K_D(S)$ is determined from K_q and the steady-state crack velocity, K_q and K_a from the static solution [38] using clip gage displacement and measured crack lengths (a_o and a_r, respectively).

In the two cases where Equation A-4 is inapplicable, limits can be set on $K_D(T)$:

(a) When the crack does not penetrate into the test section.

$$K_D(T) \leq \left(\frac{B}{b}\right)^{1/2} K_q \qquad \text{(A-5a)}$$

This was the case for specimens A-2, A-3, A-4, for all of which B = b.

(b) When the crack is not arrested and the specimen breaks completely in two, preliminary unpublished calculations by Kanninen suggest that

$$K_D(T) \leq 0.4 \left(\frac{B}{b}\right)^{1/2} K_q \qquad \text{(A-5b)}$$

This was the case for specimen A-7, for which b = 0.4B. Unfortunately, the velocity trace for this specimen was not recorded because of triggering problems.

APPENDIX B

ESTIMATION OF SIZE OF LARGEST TOLERABLE EMBRITTLED REGION IN SHIP STEEL AT NDT

Using the conservative assumption that all of the kinetic energy that is generated becomes available to drive the crack [9,36], a rapidly propagating crack will arrest whenever the total amount of strain energy made available to the crack tip becomes less than the total energy absorbed in fracture:

$$\int_{a_o}^{a_f} G\,da \leq \int_{a_o}^{a_f} \frac{K_D^2}{E}\,da \qquad \text{(B-1)}$$

where G is the strain energy release rate, a_o is the original half-crack length, and a_f is the half-crack length at arrest.

If the specimen contains an embrittled region ($K_D \simeq 0$) of width $2a_e$, and if the starting flaw size is very small, $a_o << a_f$, we can estimate the largest value of a_e consistant with crack arrest by the base metal. This value represents the largest size of embrittled region which the ship hull could contain and resist catastrophic fracture. Using the two assumptions just cited Eq. (B-1) becomes:

$$\int_{o}^{a_f} G\,da \leq \int_{a_e}^{a_f} \frac{K_D^2}{E}\,da \qquad \text{(B-2)}$$

Approximating the ship hull as an infinite center-cracked panel loaded in tension:

$$G = \frac{\sigma^2 \pi a}{E} \qquad \text{(B-3)}$$

equation (B-2) becomes:

$$\frac{\sigma^2 \pi a_f^2}{2} \leq K_D^2 (a_f - a_e) \qquad \text{(B-4)}$$

Rearranging eq. (B-4), a condition for which the crack will arrest at a half-length of a_f is defined:

$$\frac{\sigma^2 \pi a_e}{2K_D^2} \leq \frac{\left(\frac{a_f}{a_e}\right) - 1}{\left(\frac{a_f}{a_e}\right)^2} \qquad \text{(B-5)}$$

The maximum value of the right hand side of eq. (B-5) is 1/4, corresponding to $a_f = 2a_e$. If the left hand side of eq. (B-5) exceeds 1/4, the inequality is never satisfied and the crack will never arrest. Accordingly the largest tolerable size of an embrittled region is:

$$2a_e \simeq \frac{1}{\pi}\left[\frac{K_D}{\sigma}\right]^2 \qquad \text{(B-6)}$$

For ship plate, $\sigma \leq 0.5\sigma_Y$ and $\sigma_Y \simeq 300$ MNm^{-2}. Using a typical value of $K_D \simeq 100$ $MNm^{-3/2}$ at NDT, $2a_e$ becomes 140mm (5-1/2").

NONE

Security Classification

DOCUMENT CONTROL DATA - R & D

(Security classification of title, body of abstract and indexing annotation must be entered when the overall report is classified)

1. ORIGINATING ACTIVITY (Corporate author)	2a. REPORT SECURITY CLASSIFICATION
Battelle, Columbus Laboratories	UNCLASSIFIED
	2b. GROUP

3. REPORT TITLE

"Dynamic Crack Propagation and Arrest in Structural Steels"

4. DESCRIPTIVE NOTES (Type of report and inclusive dates)

Final Report - September 1971 through January 1975

5. AUTHOR(S) (First name, middle initial, last name)

George T. Hahn, Richard G. Hoagland, and Alan R. Rosenfield

6. REPORT DATE	7a. TOTAL NO. OF PAGES	7b. NO. OF REFS
January 31, 1975	52	38

8a. CONTRACT OR GRANT NO	9a. ORIGINATOR'S REPORT NUMBER(S)
N00024-72-C-5142	
b. PROJECT NO.	
c.	9b. OTHER REPORT NO(S) (Any other numbers that may be assigned this report)
d.	SSC-256

10. DISTRIBUTION STATEMENT

Distribution of this report is unlimited

11. SUPPLEMENTARY NOTES	12. SPONSORING MILITARY ACTIVITY
	Naval Ship Systems Command

13. ABSTRACT

This is the second of two Ship Structure Committee reports describing a three-year investigation of the crack propagation and arrest characteristics of ship-hull steels. The earlier report (SSC-242), which dealt principally with developmentof experimental and analytical techniques, is briefly discussed. Results are then presented for the following steels: ASTM-A517F (high strength low alloy), 9% Ni (for cryogenic service), ABS-C and ABS-E (two plates, one of which is high strength and designated EH).

The major material property affecting crack arrest is found to be the dynamic fracture toughness, K_{ID}, which is both velocity- and temperature-dependent. Expect for the 9% Ni steel, all of the materials showed an initial decrease of toughness with increasing velocity. Thus, cracks in the steels investigated here display an instability, in that propagation at higher speeds consumes progressively less energy. The negative slope of the toughness/velocity curve is particularly pronounced around the Nil-Ductility Temperatures (NDT) for the ship hull steels. At very low temperatures (e.g. -196°C), the toughness passes through a minimum and then increases with increasing velocity. It appears that this is the most general behavior for cleavage crack propagation.

In contrast, 9% Ni steel fractures by the ductile dimple mechanism and the toughness increases slightly with increasing velocity throughout the velocity range investigated.

DD FORM 1 NOV 65 1473

NONE

Security Classification

14. KEY WORDS	LINK A		LINK B		LINK C	
	ROLE	WT	ROLE	WT	ROLE	WT
Fast Fracture						
Crack Arrest						
Crack Speed						
Dynamic Fracture Energy						
Dynamic Fracture Toughness						
Arrest Toughness						
Double-Cantilever-Beam Test Specimen						
A517F Steel						
Nickel Steel						
A553 Steel						
ABS Steel						

SHIP RESEARCH COMMITTEE
Maritime Transportation Research Board
National Academy of Sciences-National Research Council

The Ship Research Committee has technical cognizance of the inter-agency Ship Structure Committee's research program:

PROF. J. E. GOLDBERG, Chairman, *School of Civil Engineering, Purdue University*
PROF. R. W CLOUGH, *Prof. of Civil Engineering, University of California*
DR. S. R. HELLER, Jr., *C'man, Civil & Mech. Eng. Dept., The Catholic Univ. of America*
MR. G. E. KAMPSCHAEFER, Jr., *Manager, Technical Services, ARMCO Steel Corporation*
MR. W. W. OFFNER, *Consulting Engineer, San Francisco*
MR. D. P. ROSEMAN, *Chief Naval Architect, Hydronautics, Inc.*
MR. H. S. TOWNSEND, *Vice President, U.S. Salvage Association, Inc.*
DR. S. YUKAWA, *Consulting Engineer, General Electric Company*
MR. R. W. RUMKE, *Executive Secretary, Ship Research Committee*

Advisory Group III, "Materials, Fabrication, and Inspection", prepared the project prospectus and evaluated the proposals for this project:

MR. G. E. KAMPSCHAEFER, Jr., Chairman, *Manager, Tech. Services, ARMCO Steel Corp.*
DR. J. M. BARSOM, *Research Consultant, U.S. Steel Corporation*
PROF. J. R. FREDERICK, *Dept. of Mech. Engineering, The University of Michigan*
MR. S. GOLDSPIEL, *Mechanical Engineer, Board of Water Supply, New York*
MR. T. E. KOSTER, *Naval Architect, AMOCO International Oil Company*
DR. J. M. KRAFFT, *Head, Mechanics of Materials Branch, Naval Research Laboratory*
MR. G. E. LINNERT, *North American Representative, The Welding Institute*
PROF. H. W. LIU, *Professor of Materials Science, Syracuse University*
PROF. W. H. MUNSE, *Dept. of Civil Engineering, University of Illinois*
MR. W. W. OFFNER, *Consulting Engineer, San Francisco*
PROF. H. C. ROGERS, *College of Engineering, Drexel University*
DR. W. F. SAVAGE, *Professor of Metallurgy, Rensselaer Polytechnic Institute*
DR. W. K. WILSON, *Analytical Mechanics, Westinghouse Electric Corporation*

The SR-201 Project Advisory Committee provided the liaison technical guidance, and reviewed the project reports with the investigator:

MR. G. E. KAMPSCHAEFER, Chairman, *Manager, Technical Services, ARMCO Steel Corp.*
DR. J. M. KRAFFT, *Head, Mechanics of Materials Branch, Naval Research Laboratory*
PROF. H. W. LIU, *Professor of Materials Science, Syracuse University*
PROF. H. C. ROGERS, *College of Engineering, Drexel University*
DR. W. K. WILSON, *Analytical Mechanics, Westinghouse Electric Corporation*

SHIP STRUCTURE COMMITTEE PUBLICATIONS

These documents are distributed by the National Technical Information Service, Springfield, Va. 22151. These documents have been announced in the Clearinghouse journal U.S. Government Research & Development Reports (USGRDR) under the indicated AD numbers.

SSC-247, *Flame Straightening Quenched-And-Tempered Steels in Ship Construction* by R. L. Rothman. 1974. AD-A 002621.

SSC-248, *Fracture Toughness Characterization of Shipbuilding Steels* by J. R. Hawthorne and F. J. Loss. 1975. AD 785034.

SSC-249, *Ship-Vibration Prediction Methods and Evaluation of Influence of Hull Stiffness Variation on Vibratory Response* by R. G. Kline and J. C. Daidola. 1975. AD-A 008388.

SSC-250, *Bibliography to Ship-Vibration Prediction Methods and Evaluation of Influence of Hull Stiffness Variation on Vibratory Response* by R. G. Kline and J. C. Daidola. 1975. AD-A 008387.

SSC-251, *A Study of Subcritical Crack Growth In Ship Steels* by P. H. Francis, J. Lankford, Jr., and F. F. Lyle, Jr. 1975. AD-A 013970.

SSC-252, *Third Decade of Research Under the Ship Structure Committee* by E. A. Chazal, Jr., J. E.Goldberg, J. J. Nachtsheim, R. W. Rumke, and A. B. Stavovy. 1976

SSC-253, *A Guide for the Nondestructive Testing of Non-Butt Welds in Commercial Ships - Part One* by R. A. Youshaw and E. L. Criscuolo. 1976.

SSC-254, *A Guide for the Nondestructive Testing of Non-Butt Welds in Commercial Ships - Part Two* by R. A. Youshaw and E. L. Criscuolo. 1976.

SSC-255, *Further Analysis of Slamming Data from the S.S. WOLVERINE STATE* by J. W. Wheaton. 1976.

SL-7 PUBLICATIONS TO DATE

SL-7-1, (SSC-238) - *Design and Installation of a Ship Response Instrumentation System Aboard the SL-7 Class Containership S.S. SEA-LAND McLEAN* by R. A. Fain. 1974. AD 780090.

SL-7-2, (SSC-239) - *Wave Loads in a Model of the SL-7 Containership Running at Oblique Headings in Regular Waves* by J. F. Dalzell and M. J. Chiocco. 1974. AD 780065.

SL-7-3, (SSC-243) - *Structural Analysis of SL-7 Containership Under Combined Loading of Vertical, Lateral and Torsional Moments Using Finite Element Techniques* by A. M. Elbatouti, D. Liu, and H. Y. Jan. 1974. AD-A 002620.

SL-7-4, (SSC-246), *Theoretical Estimates of Wave Loads On The SL-7 Containership in Regular and Irregular Seas* by P. Kaplan, T. P. Sargent, and J. Cilmi. 1974. AD-A 004554.